Aerosol and Air Quality Research, 19: 2502–2517, 2019

ISSN: 1680-8584 print / 2071-1409 online
doi: 10.4209/aaqr.2019.10.0495

$PM_{2.5}$ Associated PAHs and Inorganic Elements from Combustion of Biomass, Cable Wrapping, Domestic Waste, and Garbage for Power Generation

Zhiyong Li[1,2*], Yutong Wang[1], Songtao Guo[1], Zhenxin Li[1], Yiran Xing[1], Guoqing Liu[1], Rui Fang[1], Yao Hu[1], Hongtao Zhu[1], Yulong Yan[2]**

[1] *Hebei Key Lab of Power Plant Flue Gas Multi-Pollutants Control, Department of Environmental Science and Engineering, North China Electric Power University, Baoding 071003, China*
[2] *MOE Key Laboratory of Resources and Environmental Systems Optimization, Ministry of Education, Beijing 102206, China*

ABSTRACT

$PM_{2.5}$ fractions were collected by re-suspension of the ashes derived from the incineration processes of peanut straw (PS), wheat straw (WS), garbage-fired power plant (GFPP), domestic garbage for volume reduction (DG), and workshop of cable combustion for metal reclamation (WCC) for the analysis of 16 PAHs and 26 elements to obtain the information about their composition profiles, toxicity of PAHs, and exposure risks posed by heavy metals (HMs) and As. GFPP possessed the highest Σ16PAHs, while the lowest value occurred at DG. HMW-PAHs dominated in GFPP, while LMW-PAHs were predominant in PS and WS. BaP was the top PAH in GFPP and GFPP possessed the highest TEQ values based on the 2,3,7,8-tetrachlorodibenzodioxin (TCDD) and BaP associated TEFs, and followed by WCC > DG > WS > PS. Except for DG vs. WCC, the PAH-, and HM vs. As-profiles between any 2 out of 5 sources were different based on higher coefficients of divergence than 0.3. The sum of 10 HMs and As ($\sum_{11}$IEs) dominated in WCC due to high contents of Cu, Zn, and Pb, and followed by GFPP > DG > WS > PS. The most enriched HMs were Sb, Cu, and Pb for WCC, Sn for GFPP, and Cd for both GFPP and DG. The integrated carcinogenic risks (CRs) for children posed by both dermal adsorption (Derm) and ingestion (ING) were higher than those for adults. The CRs for children from all the 5 sources exceeded the acceptable level of 1×10^{-4}. The non-carcinogenic risks (NCRs) for children posed by both ING and DERM for 5 sources were much higher than those for adults. The NCRs for children posed by ING significantly exceeded 1, which were 63.8, 10.9, 4.11, 3.58, and 2.19 for WCC, GFPP, WS, DG, and PS.

Keywords: PAHs; Heavy metals; Cable wrapping; Garbage-fired power plant; Domestic garbage.

INTRODUCTION

Serious atmospheric quality deterioration has occurred in rapidly developing China (Fang *et al*., 2009; Pascal *et al*., 2013; Li *et al*., 2017a; Hu *et al*., 2019; Li *et al*., 2019). Zhai *et al*. (2019) reported that $PM_{2.5}$ should responsible for 1.1×10^6 excess deaths in 2015 in China. The major sources of $PM_{2.5}$ in urban areas are incomplete combustion or gas-particle conversion, and $PM_{2.5}$ contain a varied mix of chemicals inorganic ions, organic carbon and elemental carbon (Bond *et al*., 2004; Saikawa *et al*., 2009). The $PM_{2.5}$ associated organic pollutants including PAHs, PCBs, PCDD/Fs, and heavy metals were often linked with damage of health and environment (Li *et al*., 2011, 2016, 2017a, b, 2018a, b; Mario *et al.*, 2018). Exposure to high loading of atmospheric PAHs originate from both natural and anthropogenic sources is often linked with adverse health effects, especially for urban residents (Hamra *et al*., 2014; Elzein *et al*., 2019).

The $PM_{2.5}$ bounded micro-pollutants including PAHs, and heavy metals (HMs), and As could threaten the human health and endanger the ecosystem safety since their toxicity even at low levels, which had been paid more attention (Mario *et al*., 2018). China is the world's largest PAHs producer and contributes 20.1% to global emissions in 2007 (Zhang *et al*., 2019). The main emission sources of these pollutants contained incomplete combustion of fossil fuels, agricultural burning, and industrial and agricultural activities (Li *et al*., 2011, 2017a, b; Abbas *et al.*, 2018; Chen *et al*., 2018; Dat *et al*., 2018; Li *et al*., 2018a, b; Mario *et al*., 2018). The anthropogenic burning was identified as a predominant contributor to PAHs and HMs compared with the natural sources including volcanic eruptions and forest fires (Xu *et al*., 2006; Abbas *et al*, 2018).

* Corresponding author.
Tel.: +86 312 7525506; Fax: +86 312 7525506
E-mail address: lzy6566@126.com
** Corresponding author.
Tel.: +86 1061772891; Fax: +86 1061772891
E-mail address: yanyulong@yeah.net

The domestic garbage burning for volume reduction and power generation is a more concerned emission source of PAHs, dioxin, HMs, NO_x, and SO_x due to its consequent health and environmental risks (Xiang *et al*., 2013; Zhang *et al.*, 2013; Liu *et al*., 2016). As an important measure to dispose the garbage and ease the energy crisis, the garbage-fired power plant (GFPP) was widely used in the world (Murphy and McKeogh, 2004). Various air pollutants including PAHs, PCBs, and HMs originated from GFPP were more concerned and the flue gas purification technology has become a research hotspot in recent years (Consonni *et al*., 2005; Liu, 2015). Along with the increasing pressure of environment protection, especially the atmospheric environment, the family workshops located at rural areas of China aiming to metal reclamation through the burning of electric cables were closed. However, some workshops were still secretly producing at night driven by the enormous economic benefits. Huang *et al*. (1992) reported the soil adjacent to these workshops was heavily contaminated by PCBs, PAHs, PCDDs, and PCDFs. Li *et al*. (2011) also indicated that high levels of PCBs were found in soil near these workshops. China is a big agricultural country with a lots of straw produced every year, which is often directly burned in field to facilitate the cultivation in the next year (Hou *et al*., 2017). The regional air pollution events derived from biomass burning were frequently observed in recent years regardless of the strict emission limitation from Chinese government (Zhang *et al*., 2015a; Hou *et al*., 2017).

To our knowledge, few systematic studies were conducted on the $PM_{2.5}$ associated PAHs, HMs, and As originated from the combustion of biomass, garbage for power generation, cable wrapping for metal reclamation, domestic garbage for volume reduction. In this study, a sum of 42 target compounds including 16 PAHs and 26 inorganic elements were analyzed for 18 $PM_{2.5}$ samples, which were collected using re-suspension of the ashes from these related emission sources. The 16 target PAHs including naphthalene (NaP), acenaphthylene (Acy), acenaphthene (Ace), fluorine (Fl), benzo(g,h,i)perylene (BghiP), phenanthrene (Phe), anthracene (Ant), fluoranthene (FA), pyrene (Pyr), benzo(a)anthracene (BaA), chrysene (Chr), benzo(b)fluoranthene (BbF), benzo(k)fluoranthene (BkF), benzo(a)pyrene (BaP), indeno(1,2,3-cd)pyrene (Ind), and dibenzo(a,h)anthracene (DBA) were analyzed using the HP6890 GC/5973i MS with selected ion mode (SIM) in this study. The 26 inorganic elements (IEs) such as Li, Be, Na, P, K, Sc, V, Cr, Mn, Co,Ni, Cu, Zn, As, Cd, Sn, Sb, Tl, Pb, Si, Al, Ca, Mg, Fe, Ba, and Sr were analyzed by ICP-MS and ICP-OES. All of this work was to achieve the following objects: 1) the contents of PAHs and IEs in $PM_{2.5}$; 2) the PAH and IE composition profile similarity between each pair of emission sources; 3) toxicity evaluation of PAHs; and 4) the carcinogenic and non-carcinogenic exposure risks of HMs and As.

METHODOLOGY

Sample Collection and Re-suspended for Obtainment of $PM_{2.5}$

The ash samples were collected from 4 GFPPs in Hebei- and Shaanxi-Province, 4 WSs and 4 PSs in Hebei Province, 3 WCCs in Heibei Province and Tianjin city, and 3 DGs in Hebei Province during January to May, 2015. The samples were collected from the electrostatic precipitators (ESP) of garbage-fired power plants, ash outlet at bottom of the stoves, and outdoor combustion residue using a stainless shovel. Finally, 1 kg of ash was obtained and dried using a vacuum freeze dryer, and subsequently stored in brown glass bottles before re-suspended for $PM_{2.5}$ fractions.

The $PM_{2.5}$ fractions within particulate matters were collected from fly ashes using re-suspension method described in detail by Chow *et al*. (1994), Kong *et al*. (2011), and Li *et al*. (2017b). Fig. 1 was a diagrammatic sketch for sample collection using the re-suspension chamber equipped with 4 sampling channels. For each $PM_{2.5}$ sample, 10 g of ash was blow out from dust feeding bottle using a pump and entered into the re-suspension chamber and then through 4 particle size cutters (2.5 μm) and intercepted by subsequent quartz filters (QFs) (diameter 47 mm; Pall Co. USA) and Teflon membranes (diameter 47 mm; Pall Co. USA). The ash derived from one kind of fuel experienced two repeated re-suspension and finally the ash intercepted in 8 QFs was used for the analysis of 16 PAHs to ensure the detection of as many PAH isomers as possible. The ash intercepted in 2 Teflon filter was used to analyze the 26 inorganic within $PM_{2.5}$. Suspension time was set as 10 min for each sample, and then stopped running for 180 min to eliminate any interference derived from the latest experiment for sample re-suspension and collection. Prior to sampling, all the quartz filters were baked at 600°C for 2 h to eliminate the organic compounds, then equilibrated for 48 h in a room with constant temperature and humidity before and after sampling, and then weighed. The weight difference between pre- and post-sampling was used as collected $PM_{2.5}$ mass. The $PM_{2.5}$ sampling amounts were in the range of 208–1160 mg. The significant fluctuations existed among $PM_{2.5}$ yields of ashes derived from combustion of different fuels, and the maximum was possessed by peanut straw, while the minimum occurred at domestic waste.

PAHs Extraction and Analysis

The sample consists of 8 re-suspended QFs was Soxhlet extracted with actone: n-hexane (v:v = 1:1) for 24 h, concentrated by rotary vacuum evaporation, purified by a florisil column and re-concentrated to 0.5 mL under a gentle N_2 stream before analysis. The HP6890 GC/5973i MS system equipped with a DB-5 capillary column (30 m × 0.25 mm × 0.25 μm) was used to PAHs and PAEs analysis using selected ion mode (SIM). A total of 18 PAHs and 6 PAEs (DMP, DEP, DBP, DEHP, DOP, and BBP) were analyzed in this study and the corresponding PAH and PAE standards were all purchased from Dr. Ehrenstorfer GmbH (Augsburg, Germany). The 4-bromo-2-fluorobiphenyl and deuterated terphenyl (Accustandard, USA) were used as surrogate standards. D_8-NaP, D_{10}-Ace D_{10}-Phe, D_{12}-Chr, and D_{12}-Pyr supplied by Dr. Ehrenstorfer GmbH (Augsburg, Germany) were used as internal standards in analysis process. The splitless injection was adopted and Helium was used as the carrier gas with the constant flow keeping at 1.1 mL min^{-1}. The oven temperature program was as follows: 70°C held

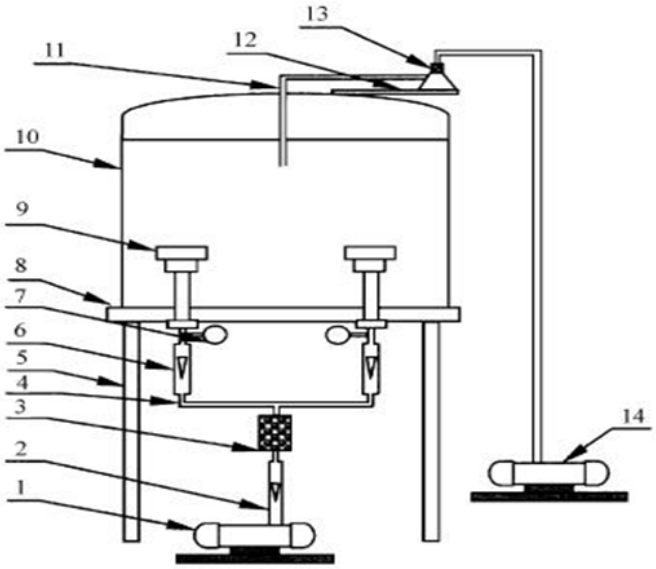

Fig. 1. Re-suspension sampling system. (1) Sampling pump, (2) Total flow meter, (3) Filter, (4) Sampling gas path, (5) Support shelf, (6) Brantch flow meter, (7) Vacuum gauge, (8) Sampling platform, (9) Stainless steel particle size cutter, (10) Re-suspension chamber, (11) Gas path of dust injection, (12) Stainless steel bottle holder, (13) Dust feeding bottle, (14) Dust feeding pump.

for 4 min, ramped to 300°C at 10°C min^{-1} and held for 2 min, and then ramped to 340°C at 5°C min^{-1}.

The limited m/z values were 129, 127 for NaP, 153, 152 for Acy, 151, 153 for Ace, 165, 167 for Fl, 179, 176 for Phe and Ant, 101, 203 for Flu and Pyr, 229, 226 for BaA, 226, 229 for Chr, 256, 126 for BbF and BkF, 253, 126 for BaP and BeP, 138, 227 for Ind, 139, 279 for DBA, 138, 227 for BghiP, 150, 301 for COR, respectively. The m/z values as 128, 154, 152, 166, 178, 178, 202, 202, 228, 228, 252, 252, 252, 252, 276, 278, 276, 300 were selected to quantify the NaP, Acy, Ace, Fl, Phe, Ant, Flu, Pyr, BaA, Chr, BbF, BkF, BaP, BeP, Ind, DBA, BghiP and COR, respectively. The correspondingly limited m/z values and quantitative m/z values (in bracket) were 68 and137 (136) for D_8-NaP, 162 and 165 (164) for D_{10}-Ace, 94 and 189 (188) for D_{10}-Phe, 120 and 241 (240) for D_{12}-Chr, and 260 and 265 (264) for D_{12}-Pyr, respectively. The surrogate standards 4-bromo-2-fluorobiphenyl and deuterated terphenyl possessed the corresponding values as 170 and 151 (250), and 122 (244).

The PAH pre-treatment and analysis were entirely conducted according to the strict quality assurance (QA) and quality control (QC) procedures. The experiments associated with sample and procedure blank, sample duplication, and recoveries of matrix spiked and internal standards were carried on schedule every 6 samples. Sample and procedure blank experiments showed that no target chemicals were detected. The recovery rates ranged from 72.5 to 121% for 4-bromo-2-fluorobiphenyl and from 75.3 to 122% for deuterated terphenyl, and the mean values were 96.3% and 90.9%, respectively. The 18 PAHs in 3 matrix injected samples possessed the recovery fluctuated from 72.0% for Acy to 118% for Pyr with the mean value as 93.5 ± 9.96% and the mass concentrations of 16 PAHs corresponding to triple signal to noise ratio were identified as the method detection limits (MDLs) of them. The corresponding MDLs for 16 PAHs (in ng g^{-1}) ranged from 0.06 for BaP to 0.44 for Fl with a mean as 0.18 ± 0.11.

Analysis of $PM_{2.5}$ Associated Inorganic Elements

Among the 26 inorganic elements (IEs), 19 IEs including Li, Be, Na, P, K, Sc, V, Cr, Mn, Co, Ni, Cu, Zn, As, Cd, Sn, Sb, Tl, and Pb were analyzed by ICP-MS (Agilent 7500a, Agilent Co. USA), and the rest 9 IEs such as Si, Al, Ca, Mg, Fe, Ba, and Sr were analyzed by ICP-OES system (Agilent 5100, Agilent Co. USA). The same analyzed method was detailed documented by Li *et al*. (2017a, b) and simplified as follows. For ICP-MS, the 1 Teflon filter was heated with 5 mL of aqua regia (V:V = 1:5) and 1 drop of HF acid (V:V = 1:1) at 120℃ for 2 h, and then raised to 130℃ until dryness. Then the HCl acid was added and heated for 20 mins, and the extracts were transferred into a plastic comparison tubes before analysis. For ICP-OES analysis, the other 1 Teflon filter was cut into pieces and heated at 300℃ for 40 mins, and gradually raised to 530–550℃ for completely ashing. Several drops of absolute ethanol and 0.1–0.2 g of NaOH were added and heated at 500℃ for 10 mins, and the water was added and boiled. Finally the extract combined with 2 mL HCl and diluted to 10 mL before analysis.

The method detection limits (MDLs) for 26 IEs were ranged from 0.10 ng of Be to 1810 ng of Fe. The relative standard deviation (RSD) values for 26 elements were 2.12%, 2.51%, 2.57%, 3.12%, 1.77%, 2.58%, 3.01%, 4.55%, 5.80%, 2.43%, 2.23%, 3.22%, 4.28%, 1.72%, 2.58%, 3.02%, 4.28%, 5.15%, 3.58%, 2.12%, 2.57%, 3.25%, 4.43%, 4.59%, 6.15%, and 2.77%, respectively. The standard soil materials GBW07446-GBW07457 (Center for National Standard Matter, China) were used to determine the accuracy of ICP-MS and ICP-OES.

RESULTS AND DISCUSSION

Contents of $PM_{2.5}$ Associated PAHs

The $PM_{2.5}$ fractions of the ashes originated from five combustion sources differed significantly from each other in their Σ_{16}PAHs concentrations. GFPP possessed the highest Σ_{16}PAHs as 66500 ± 9800 ng g^{-1}, while the minimum occurred at DG and it was 2480 ng g^{-1}. The Σ_{16}PAHs values (in ng g^{-1}) of rest 3 combustion sources conformed to the order WS (13600 ± 1980) > WCC (9890 ± 1280) > PS (3570 ± 852). All the five combustion sources possessed much higher levels of PAHs than those of 12 wood pellets burning (0.064 – 0.90 mg kg^{-1}) (Orecchio *et al*., 2016). For biomass fuels, the Σ_{16}PAHs values for $PM_{2.5}$ from PS- and WS-burning were significantly higher than 65.0 – 1310 ng g^{-1} for the five-sized parts of bottom ashes from 8 kinds of bio-fuels in Beijing-Tianjin-Hebei region, China (Li *et al*., 2018a). Compared with the other similar studies, the $PM_{2.5}$ bounded PAHs from the GFPP in this study were much higher than 21.9 ng g^{-1} of fly ashes from the 16 Chinese coal-fired power plants with the individual unit as 600 MW (Li *et al*., 2016), 29.8–63.8 ng g^{-1} for bottom ashes and 3860–148991 ng g^{-1} for fly ashes from 48 biomass-fired power plants in Czech Republic (Zdeněk *et al*., 2016), 2830–5320 ng g^{-1} for fly ashes and 930–2080 ng g^{-1} for fly ashes from a Chinese coal-fired plant with the individual unit as 300 MW (Wang *et al*., 2013), 1200–5900 ng g^{-1} for bottom ashes from the municipal solid waste (MSW) burning (Peng *et al*., 2016a), 1970–3710 ng g^{-1} for bottom ashes from the hydrothermally treated MSW burning (Peng *et al*., 2016b), 13540 ng g^{-1} for fly ash formed during the burning process of pressurized coal (Zhou *et al*., 2009), and 31–2160 ng g^{-1} for fly ashes from 4 bio-fueled power plants in India (Masto *et al*., 2015). For biomass combustion process, the WS and PS possessed higher values than those of the bio-fueled power plants in Czech Republic (Zdeněk *et al*., 2016) and India (Masto *et al*., 2015), which possibly owning to the more complete combustion of biomass in the industrial boilers (Li *et al*., 2016, 2017b). The bottom ashes possessed higher TOC values compared than those of fly ashes, so the PAHs in bottom ashes were higher than those of fly ashes. Li *et al*. (2017b) reported that the sum of 18 PAHs in bottom ashes from burning of 8 types of bio-fuels were in the range of 65–1310 ng g^{-1}. The PAHs preferred to enrich in finer particles during the combustion process (Kong *et al*., 2011; Masto *et al*., 2015; Li *et al*., 2016, 2017b). In addition to the combustion completeness and ash particle size, fuel type was another important influence factor on PAH emissions (Kong *et al*., 2011; Masto *et al*., 2015; Li *et al*., 2016, 2017b).

Fig. 2 showed the PAH ring-size distributions in $PM_{2.5}$ fractions within 5 kinds of ashes. The PAHs were divided to three classes as low molecular weight (LMW) PAHs, medium molecular weight (MMW) PAHs, and high molecular weight (HMW) PAHs based on their molecular weight (Kong *et al*., 2011; Li *et al*., 2016, 2018a). The 2- and 3-ring compounds were identified as LMW-PAHs, 4-ring compounds were contained in medium molecular weight (MMW) PAHs, and 5-, 6-, 7-ring compounds were included in HMW PAHs. The contributions of differently sized PAHs varied significantly among the 5 combustion sources. The LMW PAHs dominated in $PM_{2.5}$ from burning of the biomass including PS and WS and contributed 82.5 ± 8.56% and 91.6 ± 9.78% to the total PAHs in them. The similar results were found for the bottom ashes from combustion of 6 types of straws in Beijing-Tianjin-Hebei region, and the LMW-PAHs accounted for 78.3%, 80.2%, 92.5%, 69.3%, 96.4%, and 96.7% to the total PAH concentrations in bottom ashes from burning of the straws of soybean, millet, walnut, cotton,

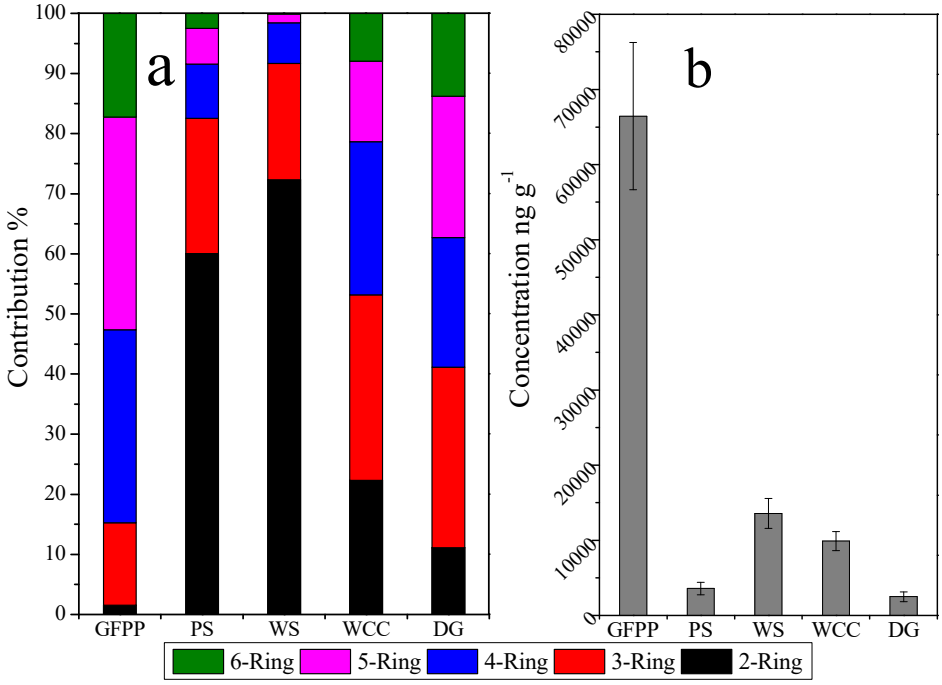

Fig. 2. Ring size distribution and concentration of the $PM_{2.5}$ bounded PAHs from 5 combustion sources.

corn, and corn cob, respectively (Li *et al*., 2018a). Also the LMW-PAHs contributed 86.9% to the total PAHs in fly ashes from 4 Indian biomass-fired power plants (Masto *et al*., 2015), while relatively low contributions of 32.7% and 44.5% were reported for the phytomass- and dendromass-fueled power plants in Czech Republic (Košnář *et al*., 2016). However, HWM-PAHs dominated in $PM_{2.5}$ from GFPP and contributed 52.6 ± 5.11% to the total PAHs, and the LMW-PAHs only contributed 15.3 ± 2.86% to the total PAHs. For DG and WCC, the LMW- and MMW-PAHs occupied a considerable proportion in the total PAHs.

PAH Composition Profiles in $PM_{2.5}$ from Five Combustion Sources

Fig. 3 listed the contents of individual PAH congener in $PM_{2.5}$ for all the 5 burning sources. The 16 PAH congeners were detectable among all the $PM_{2.5}$ samples in this study. The mean mass concentrations (in ng g^{-1}) of the top 6 PAHs followed the order of BaP (10600) > Chr (7640) > BkF (5970) > Ind (5740) > BghiP (5730)> Phe (5480) for GFPP, while they were NaP (2200) > Phe (2070) > Flu (920) > Pyr (705) > BbF (634) > BaP (492) for WCC, Phe (500) > NaP (275) > BbF (266) > BaP (250) > InD (189) > Flu (175) for DG, NaP (2140) > Phe (657) > Flu (157) > BbF (120) > Pyr (90.4) > BaP (57.8) for PS, and NaP (9810) > Phe (2280) > Flu (487) > Pyr (262) > Ant (187) > Chr (127) for WS, respectively.

Different PAH profiles among different combustion sources were documented elsewhere. The indoor burning of biomass in India caused the emissions of top PAHs such as Ant, Flu, BaA, and Chr (Singh *et al*., 2013). Masto *et al*. (2005) indicated that the predominant PAHs NaP, Phe, BbF, and Flu were found in the bottom ashes from 38 Indian biomass-fired power plants, which was similar to those of PS and WS in this study. Orecchio *et al*. (2016) reported the top PAHs for wood pellet burning for heating in Italy, which were NaP, Phe, and Ant for burning of fir, NaP, Phe, and Flu for burning of the mixture of fir and beech, and NaP, Phe, and Acy for conifers, respectively. In this study, the burned cable wrapping in the metal reclamation workshops contained polyvinyl chloride (PVC), polyethylene (PE), polyperfluoroethylene propylene (PPFEP), polyolefin (PO), chlorinated polyethylene (CPE), chloroprene rubber (CPR), silicon rubber (SR), and chlorosulfonated polyethylene (CSPE). The dominated PAHs derived from burning of the aforementioned mixed materials were NaP, Phe, Flu, Pyr, BbF, and BaP. The predominant PAHs in 12 target PAHs as NaP, BkF, and Ant for polystyrene, NaP, Ant, and Chr for PVC, NaP, Fl, and Phe for low density PE, NaP, Phe, and Fl for high density PE, and NaP, Ace, and Fl for polypropylene and polyethyleneterephthalate were reported by Valavanidis *et al*. (2008). The different plastic materials, target PAHs, and ash sizes between two studies brought about the difference of PAH profiles.

A widely known parameter as coefficient of divergence (CD) documented elsewhere was applied to distinguish the

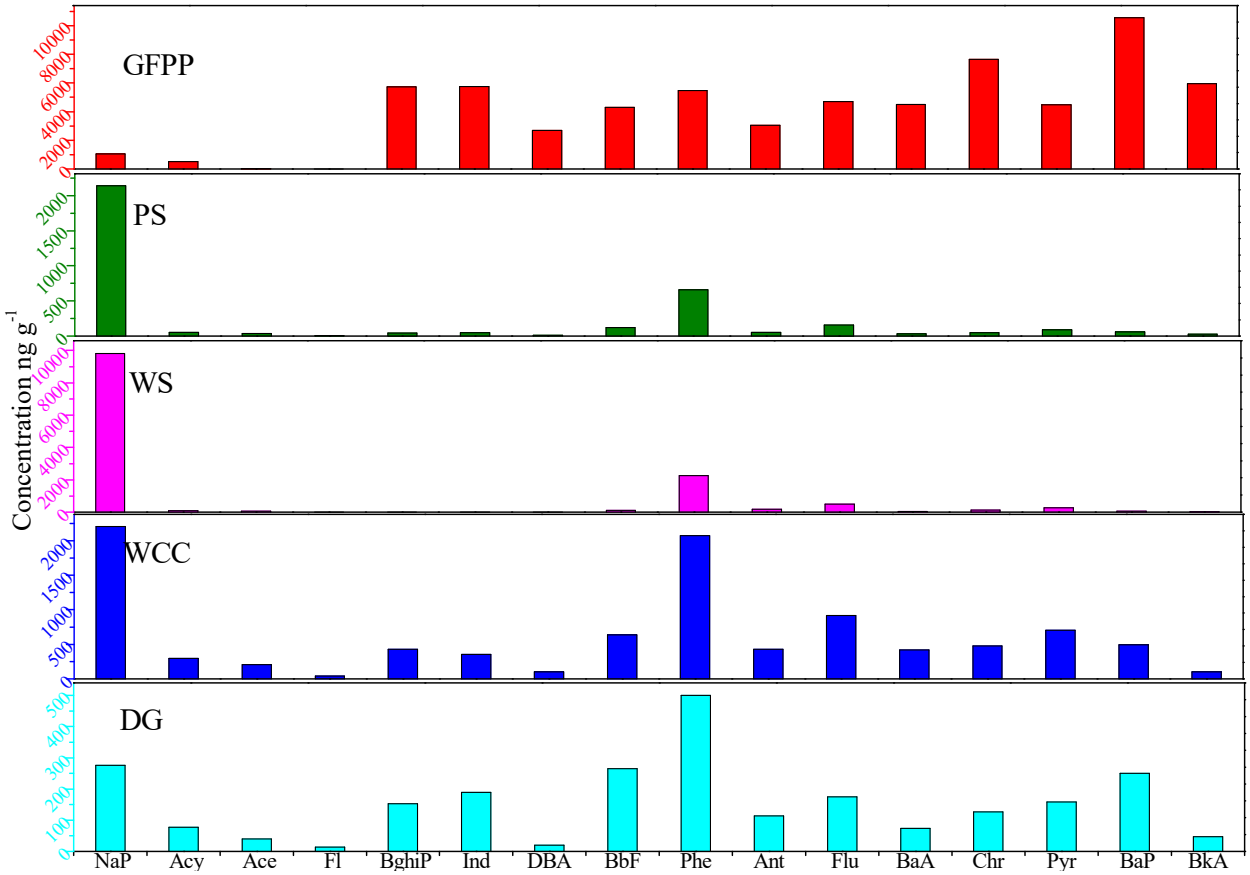

Fig. 3. Composition profiles of PAHs for five combustion sources.

similarity of PAH profiles between two emission sources (Kong *et al*., 2011; Li *et al*., 2016, 2017b, 2018b). CD value was calculated as follows:

$$CD_{jk} = \sqrt[2]{\frac{1}{p} \times \sum \left(\frac{x_{ik} - x_{ij}}{x_{ik} + x_{ij}} \right)^2} \quad (1)$$

where p is the number of the target compounds detected for each source, x_{ij} and x_{ik} are the normalized concentration of i^{th} PAH in source j and k. The CD value approaches zero indicated the profile similarity between two sources, while the CD value of one suggested the difference of PAH profiles (Wongphatarakul *et al*., 1998; Kong *et al*., 2011; Li *et al*., 2016, 2017b, 2018b). The critical CD value of 0.3 used in identification of source profile similarity was documented frequently in recent studies (Kong *et al*., 2011; Li *et al*., 2016, 2017b, 2018a, b).

Except for the lower CD value of WCC vs. DG (0.20 ± 0.05), the CD values for any two sources were higher than 0.3 and they were 0.70 ± 0.15, 0.78 ± 0.11, 0.55 ± 0.09, 0.51 ± 0.08, 0.48 ± 0.06, 0.46 ± 0.06, 0.53 ± 0.10, 0.71 ± 0.21, and 0.73 ± 0.19 for GFPP vs. PS, GFPP vs. WS, GFPP vs. WCC, GFPP vs. DG, PS vs. WS, PS vs. WCC, PS vs. DG, WS vs. WCC, and WCC vs. DG, respectively (Fig .4). The results showed that the PAH profiles for both WCC and DG were similar, while the rest 9 pairs of combustion sources were all different each other (Kong *et al*., 2011; Li *et al*., 2016, 2017b, 2018b). The similarity of PAH profiles between WCC and DG was possibly resulted from the similar common principle component of plastics between two fuels.

The difference of mass fractions for NaP and Phe in the total PAHs among the 5 kinds of sources was a common cause for the difference of PAH profiles for all the 9 pairs of sources (Fig. 5). Special cases existed between each pairs of sources, BbF and Pyr were the perpetrators for PAH profile difference between WS and PS, BkF, BghiP, and BaA were the contributors to the profile difference between GFPP and WS, and the profile difference between DG and WS were mainly attributed to BbF, BaP, and Ind.

Potential Health Risk Assessment for $PM_{2.5}$ Bounded PAHs

Widely known parameters such as toxicity equivalent concentration (TEQ) based on 2,3,7,8-tetrachlorodibenzodioxin (TCDD), BaP-based equivalent contribution (BaPeq), total carcinogenic PAHs (C-PAHs), and BaP-based equivalent carcinogenic power (BaPE) (Kong *et al*., 2011; Cheruiyot *et al*., 2015; Li *et al*., 2016; Tiwari *et al*., 2017; Li *et al*., 2018a). Total toxicity equivalency (TEQ) based on TCDD for the 16 PAHs were calculated as $TEQ = \Sigma PAH_i \times TEF_i$ and the toxicity equivalent factors (TEFs) were same as reported values by Nisbet and LaGoy (1992), and they were 0.001, 0.001, 0.001, 0.001, 0.001, 0.01, 0.001, 0.001, 0.1, 0.01, 0.1, 0.1, 1, 0.1, 1, and 0.01 for NaP, Acy, Ace, Fl, Phe, Ant, Flu, Pyr, BaA, Chr, BbF, BkF, BaP, Ind, DBA, and BgP, respectively. The BaPeq was calculated by Eq. (2) and the relative BaP based TEF values were found in Liu *et al*. (2009).

$$BaPeq_i\,(\%) = \frac{PAH_{i,TEF} \times PAH_i}{PAH_{Bap,TEF} \times PAH_{Bap}} \times 100\% \quad (2)$$

where $PAH_{i,TEF}$ is the BaP based TEF for the i^{th} individual PAH, PAH_i is the concentration for individual PAH in $PM_{2.5}$,

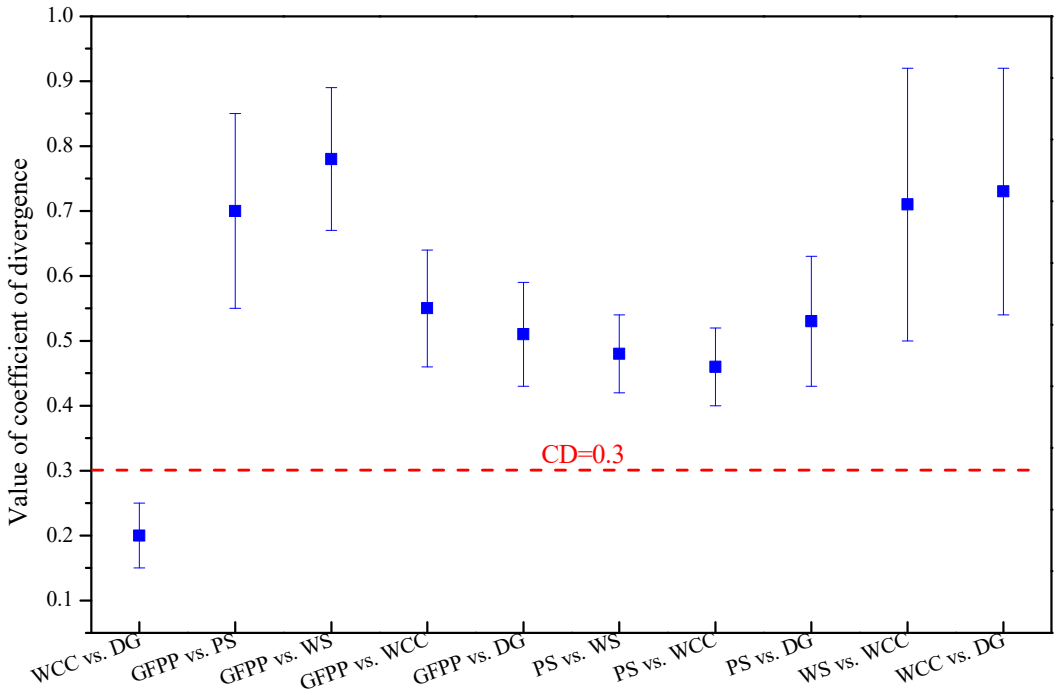

Fig. 4. Coefficients of divergence for the ten pairs of pollution sources.

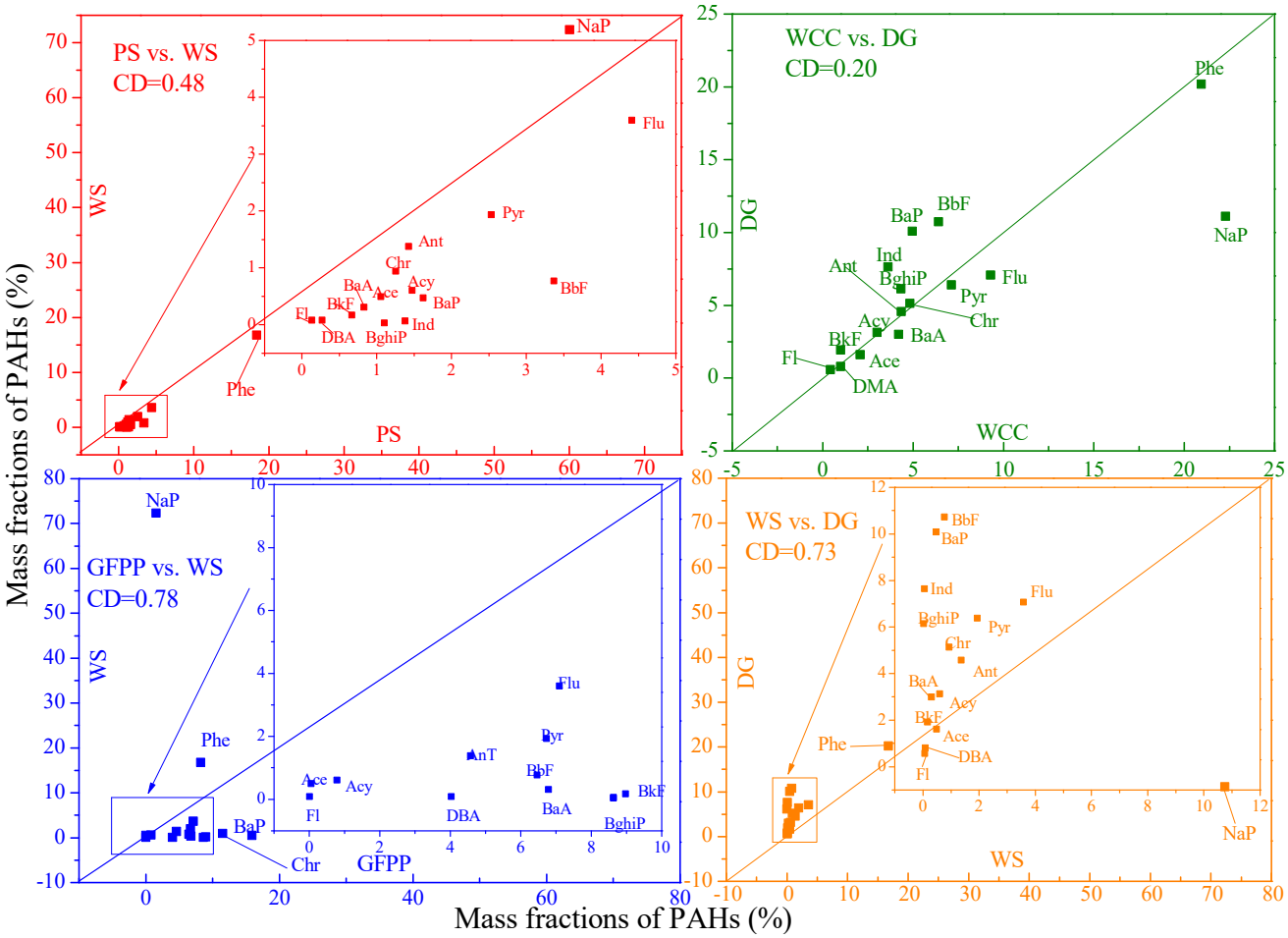

Fig. 5. Values of coefficient of divergence of PAHs for four pairs of sources.

$PAH_{i,TEF}$ is the BaP based TEF for the i^{th} PAH and it is referred to Liu *et al*. (2009), $PAH_{BaP,TEF}$ is equal to 1, which is the BaP TEF, and PAH_{BaP} is the BaP concentration of $PM_{2.5}$ associated BaP. BaPE (reported in ng g^{-1}) is calculated as BaA × 0.06 + B[b,k]F × 0.07 + BaP + DBA × 0.6 + Ind × 0.08 (Liu *et al*., 2009; Li *et al*., 2016, 2018a). C-PAHs is the sum of mass concentrations for all the 7 carcinogenic PAHs including BaA, Chr, BbF, BkF, BaP, Ind, and DBA.

The results related to BaPE, TEQ, BaPeq, and C-PAHs for $PM_{2.5}$ from 5 types of ashes were listed in Table 1. BaPeq contributions of each PAH were highly volatile among the five kinds of sources depend on the significant fluctuation of their concentrations and BaP-based toxicity equivalent factors, and the similar status was found in Li *et al*. (2016, 2018a). For GFPP, the top contributors of BaPeq were DBA, Ind, BbF, and BkF, while they were Flu, DBA, BbF, and Chr for WS, BbF, DBA, Flu, and Ind for PS, BbF, DBA, Ind, and Flu for DG, and DBA, BbF, Flu, and Ind for WCC. GFPP possessed the highest C-PAHs concentration of 41.4 μg g^{-1}, while the PS had the minimum value as 0.35 μg g^{-1}, and the C-PAHs values (in μg g^{-1}) of 2.58, 0.97, and 0.38 were attributed to WCC, DG, and WS, respectively. The BaP concentration as high as 10600 ng g^{-1} for GFPP should be paid more attentions. The similar results were found between the TEQ concentrations based on TCDD associated TEFs and BaPeq values for the five sources. TEQ values (in ng g^{-1}) for the 5 sources followed the order GFPP (15500) > WCC (761) > DG (332) > WS (109) > PS (94.3), and they were GFPP (15400) > WCC (778) > DG (336) > WS (119) > PS (97.2) for BaPeq concentrations (in ng g^{-1}) of five sources. The GFPP possessed the highest values of TEQ and BaPeq due to its highest BaP concentrations combined with the high TEF values, while biomass burning including PS and WS resulted in the lowest ones. In regard to the BaPE (in ng g^{-1}), the same trend with both TEQ and BaPeq was found, which was GFPP (13600) > WCC (656) > DG (303) > WS (82.9) > PS (79.4).

Concentrations and Exposure Risks of Inorganic Elements

The total contents of 26 IEs (Σ_{26}IEs) fluctuated from 154000 μg g^{-1} for DG to 483000 μg g^{-1} for GFPP, and they were 409000 for PS, 367000 for WS, and 320000 for WCC, respectively. Fig. 6 listed the contents for each of 26 IEs for five sources. K dominated in $PM_{2.5}$ derived from PS- and WS-burning, which was similar to the reported result by Li *et al*. (2017b). K was always used as a marker for biomass burning (Duan *et al*., 2004). K contributed 8.02% and 14.7% to the $PM_{2.5}$ mass from PS and WS, and the obvious fluctuation between PS and WS was attributed to the difference of plant physiological characteristics and local soil characteristics (Duan *et al*., 2004; Wang *et al*., 2016).

Table 1. BaPeq and BaPE for $PM_{2.5}$ from the five sources and BaPeq ratios for the individual PAH congener.

PAHs	[a]TEF	BaPeq (%)				
		GFPP (n = 4)	WS	PS	DG	WCC
Phe	0.0005	0.03 ± 0.01	1.77 ± 0.11	0.57 ± 0.08	0.10 ± 0.02	0.21 ± 0.04
Ant	0.0005	0.01 ± 0.00	0.15 ± 0.03	0.04 ± 0.00	0.02 ± 0.00	0.04 ± 0.01
Flu	0.05	2.23 ± 0.61	38.0 ± 5.26	13.6 ± 4.50	3.50 ± 0.71	9.35 ± 1.87
Pyr	0.001	0.04 ± 0.01	0.41 ± 0.08	0.16 ± 0.03	0.06 ± 0.02	0.14 ± 0.05
BaA	0.005	0.21 ± 0.06	0.33 ± 0.06	0.26 ± 0.04	0.15 ± 0.04	0.42 ± 0.08
Chr	0.03	2.17 ± 0.12	5.95 ± 0.88	2.32 ± 0.08	1.53 ± 0.61	2.91 ± 0.90
BbF	0.1	4.07 ± 0.92	16.2 ± 3.02	20.8 ± 4.02	10.6 ± 2.01	12.9 ± 3.33
BkF	0.05	2.83 ± 0.75	1.75 ± 0.52	2.07± 0.71	0.95 ± 0.12	1.01 ± 0.15
BaP	1.00	100 ± 0.00	100 ± 0.00	100 ± 0.00	100 ± 0.00	100 ± 0.00
Ind	0.1	5.44 ± 2.22	1.32 ± 0.41	8.53 ± 1.02	7.57 ± 1.51	7.27 ± 2.22
DBA	1.1	27.9 ± 8.21	19.2 ± 3.66	18.5 ± 3.78	8.73 ± 1.85	22.2 ± 4.00
BghiP	0.02	1.09 ± 0.54	0.13 ± 0.05	1.36 ± 0.51	1.22 ± 0.39	1.74 ± 0.56
C-PAHs (μg g^{-1})		41.4 ± 9.36	0.38 ± 0.09	0.35 ± 0.10	0.97 ± 0.14	2.58 ± 0.44
BaPE (ng g^{-1})		13600 ± 1520	82.9± 8.56	79.4 ± 11.2	303 ± 75.2	656 ± 98.8
BaPeq (ng g^{-1})		15400 ± 2100	119 ± 21.0	97.2 ± 11.0	336 ± 49.8	778 ± 78.9
TEQ[b] (ng g^{-1})		15500 ± 2190	109 ± 22.0	94.3 ± 13.2	332 ± 51.1	761 ± 69.8

[a] TEF values based on BaP.
[b] TEQ calculated based on TCDD associated TEF.

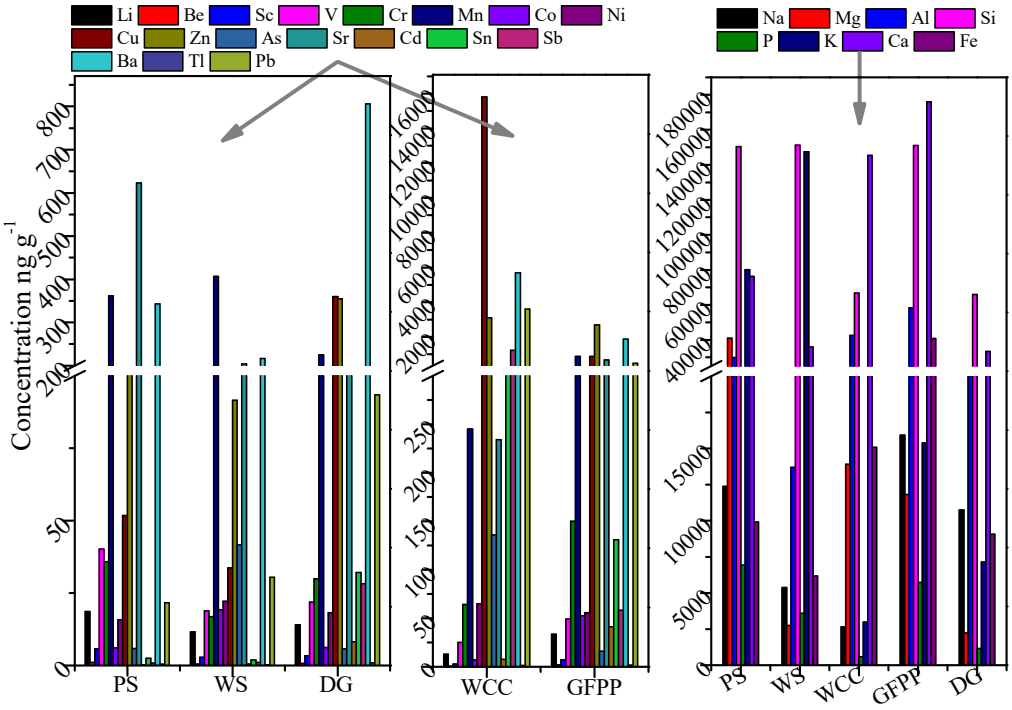

Fig. 6. Mean content of the individual element for five combustion sources.

The IEs were often divided into three classes based on their contents: 1) IEs with high contents including Al, Si, Ca, K, Mg, Fe, P, and Ti; 2) IEs with medium contents such as Mn, Na, Zn, Cu, Sr, Zr, Rb, Pb, and Mo; and 3) IEs with lower contents containing Sc, Li, V, Cr, Ni, Co, Sb, As, Y, Cs, Bi, Tl, Th, Sn, Cd, La, Ce, Sm, W, and U (Li *et al.*, 2017b). The top 9 IEs with higher contents were Si > K > Ca > Mg > Al > Na > Fe > P for PS, Si > K > Ca > Al > Fe > Na > P > Mg > Mn for WS, Ca > Si > Al > Cu > Fe > Mg > Ba > Pb > Zn for WCC, Ca > Si > Al > Fe > Na > K > Mg > P > Zn > Ba for GFPP, and Si > Ca > Al > Na > Fe > K > Mg > P > Ba for DG, respectively. PS and WS possessed higher K contents (80.2 and 147 mg g^{-1}) than the corresponding 2.98 mg g^{-1} for WCC, 15.4 mg g^{-1} for GFPP, and 7.14 mg g^{-1} for DG, K namely as an important nutrient element of plants would be the explanation. The highest Cu of 15.8 mg g^{-1} was found for WCC compared with the 0.05 mg g^{-1} for PS, 0.03 mg g^{-1} for WS, 0.89 mg g^{-1} for GFPP, and 0.36 mg g^{-1} for DG. Cu was the main component in wire, which caused the high level of Cu in $PM_{2.5}$ from WCC.

HMs and As were more concerned than the other elements in their seriously adverse health effects to people (Li *et al.*, 2017a, b; Hu *et al.*, 2019). In this study, the 10 HMs (e.g., Zn, Mn, Cu, Pb, Co, Ni, V, Cr, Cd, Sn) and As most concerned were all detected. The sum of these 11 inorganic elements ($\sum_{11}$IEs) dominated in WCC due to its high contents of Cu, Zn, and Pb, which was 23.4 ± 2.88 mg g^{-1}. The $\sum_{11}$IEs (reported in mg g^{-1}) followed the order as GFPP (5.44 ± 0.65) > DG (1.16 ± 0.06) > WS (0.68 ± 0.09) > PS (0.63 ± 0.05). The individual HM and As varied significantly among different sources, they were Mn > Zn > Cu >V > Cr > Pb > Ni > Co > As > Sn > Cd for PS, Mn > Zn > As > Cu > Pb > Ni > Co > V > Cr > Sn > Cd for WS, Cu > Pb > Zn > Sn > Mn > As > Ni > Cr > V > Cd > Co for WCC, Zn > Cu > Mn > Pb > Cr > Sn > Ni > Co > V > Cd >As for GFPP, and Cu > Zn > Mn > Pb > Sn > Cr > V > Ni > Cd > Co > As for DG, respectively. The highest levels of Cu, Zn, Sn, and Pb were found in $PM_{2.5}$ from WCC.

Also the similarity of HM vs. As profiles between each pair of combustion sources were evaluated using the CD values. Except the lower CD of 0.21 than 0.3 was found for GFPP vs. DG, the other pairs of sources possessed the higher CD values than 0.3, which were 0.36 for PS vs. WS, 0.72 for PS vs. WCC, 0.55 for PS vs. GFPP, 0.51 for PS vs. DG, 0.76 for WS vs. WCC, 0.60 for WS vs. GFPP, 0.58 for WS vs. DG, 0.68 for WCC vs. GFPP, and 0.67 for WCC vs. DG. Aforementioned CD values indicated the HMs and As profiles for all the pairs of sources except for GFPP vs. DG differed from each other. Fig. 7 listed the CD values of HMs vs. As profiles for four pairs of combustion sources. In generally, the difference of mass fractions of Zn, Mn, Pb, As, and Cu weaken the similarity of HM vs. As profiles between two sources.

Enrichment Factors and Igeo Values of Heavy Metals and As

A widely known parameter namely as enrichment factor (EF) was used to identify the IE was derived from human activities or natural processes, and further access the extent of anthropogenic impact (Li *et al.*, 2017a, b). The IE possessed EF close to 1 indicated its crustal origin, while EF higher than 10 implied the significantly anthropogenic influence. In this study, EFs were used to identify the influence of $PM_{2.5}$ associated IEs on local soil and air. EF was obtained by the following equation:

$$EF = \frac{\left(C_n / C_{ref}\right)}{\left(B_n / B_{ref}\right)} \tag{3}$$

where C_n is the measured content of the target IE in $PM_{2.5}$, C_{ref} is the measured content of reference IE in $PM_{2.5}$, B_n is the background content of the target IE in local soil, and B_{ref}

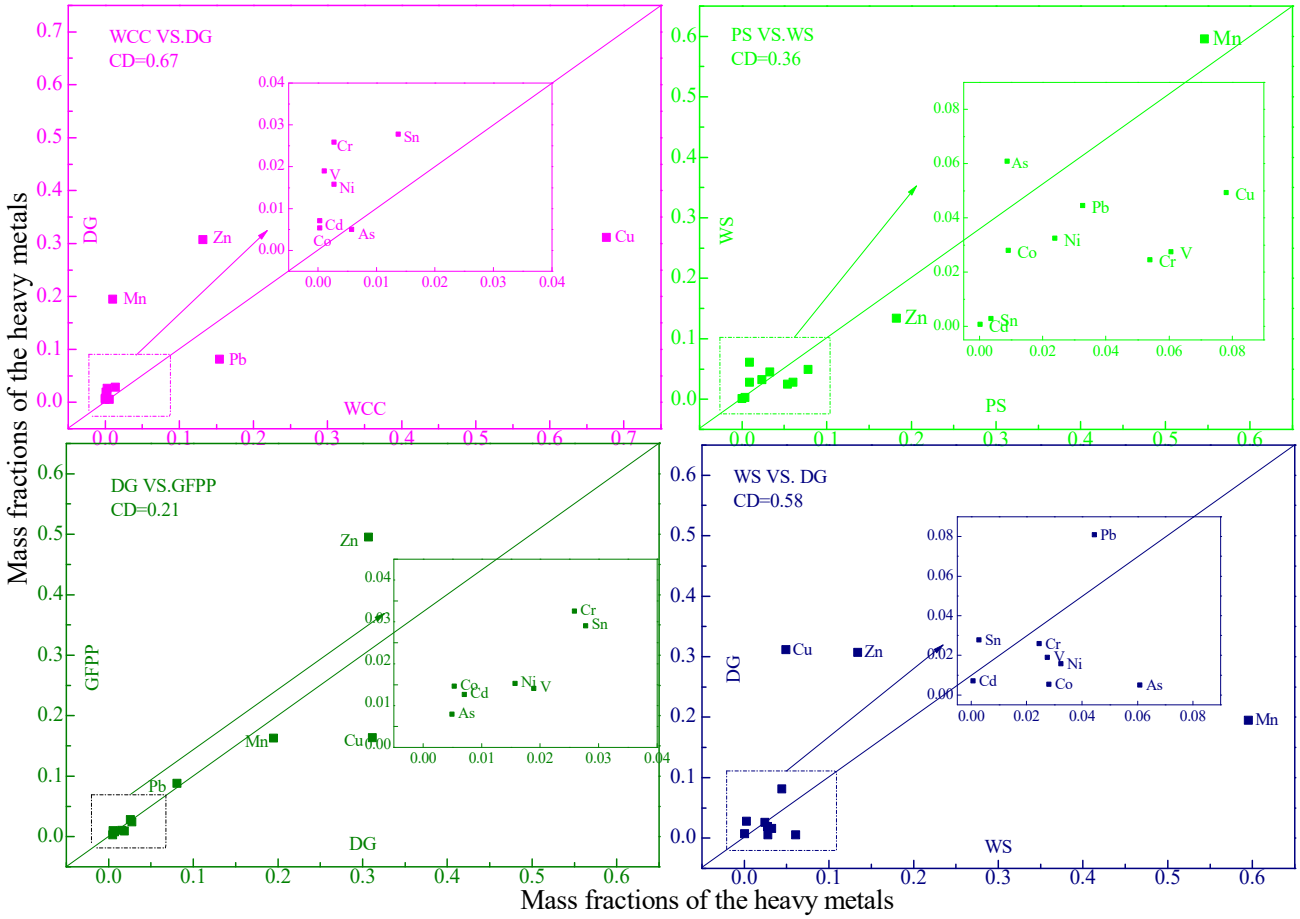

Fig. 7. Values of coefficient of divergence of HMs and As for four pairs of sources.

is the background content of reference IE in local soil. Al was always selected as reference element in related studies of China, and Al was also used as reference element in this study (Li *et al*., 2017a, b). The EF values for the individual IE varied among different sources or the same source (Table 2). K was more enriched in biomass fuel such as PS and WS, Sb, Cu, and Pb were more inclined to enrich in WCC, Sn was preferential enrichment in WCC and GFPP, and Cd intended to enrich in GFPP and DG. Sb and Cu in WCC possess higher EFs as 160 and 114, which suggested the significant influence of human activities.

Geo-accumulation index (Igeo) had been widely used in IEs related studies (Kong *et al*., 2011; Li *et al*., 2013; Li *et al*, 2017a, b), which was calculated as follows:

$$Igeo = \log_2(C_n/1.5B_n) \quad (4)$$

where C_n and B_n are measured content and soil background content of the target element, and the constant of 1.5 is used to evaluate the natural fluctuation of the target element and assess the slightly anthropogenic impact (Wei *et al*., 2009). The Igeo values of ≤ 0, 0–1, 1–2, 2–3, 3–4, 4–5, and > 5 indicate uncontaminated, uncontaminated to moderately contaminated, moderately contaminated, moderately to heavily contaminated, heavily contaminated, heavily to extremely contaminated, and extremely contaminated, respectively. Table 3 listed the Igeo values for 24 IEs in $PM_{2.5}$ generated from five combustion sources.

In regard to the more concerned HMs and As, Sb, Cu, Pb, Sn, and Cd in $PM_{2.5}$ from WCC owned the Igeo values as high as 9.66, 9.18, 7.07, 6.63, and 6.01, which indicated that these HMs were extremely contaminated. Zn and As from WCC also had high Igeo values as 4.98 and 3.00. For GFPP, Cd, Sn, Sb, and Cu possessed higher Igeo values than 5, which were 8.46, 6.57, 5.12, and 5.05 indicating extreme contamination for them. Zn and Pb from GFPP had high Igeo values as 4.96 and 4.17 implying they were heavy to extreme contamination. Cd from DG also was extreme contamination based on its high Igeo value of 6.12.

Exposure Risks of Heavy Metals and As for Five Combustion Sources

EPA Human Health Risk Assessment Guidance (2009) provided information and methods to assess the impact on human health of toxic substances released into environment. The same assumptions were adopted as Mejido in 2017 and briefly stated as follows: 1) The exposure population was restricted to local residents and divided into children (≤ 6 years) and adults (≥ 21 years); 2) Three possible exposure pathways were involved including direct inhalation, dermal adsorption, and ingestion through food and drink containing deposited particles; 3) The intake rates approach those developed for soil (Mejido *et al*., 2017). The daily intake by ingestion, dermal adsorption dose, and exposure concentration by inhalation labeled as CDI_{ing} (mg kg^{-1} day^{-1}), DAD_{derm} (mg^{-1} kg^{-1} day^{-1}), and EC_{inh} (μg m^{-3}) are calculated as following expressions:

$$CDI_{ing} = \frac{C \times IngR}{BW} \times \frac{EF \times ED}{AT} \times CF \quad (5)$$

Table 2. Enrichment Factors of inorganic elements for 5 combustion sources.

	PS	WS	WCC	GFPP	DG
Li	0.18 ± 0.02	0.24 ± 0.01	0.09 ± 0.02	0.13 ± 0.03	0.18 ± 0.05
Be	0.12 ± 0.03	0.13 ± 0.03	0.04 ± 0.01	0.09 ± 0.02	0.11 ± 0.03
Na	1.90 ± 0.62	1.80 ± 0.65	0.28 ± 0.10	1.57 ± 0.52	2.21 ± 0.69
Mg	10.6 ± 2.10	1.55 ± 0.45	2.53 ± 0.75	1.39 ± 0.38	0.77 ± 0.22
Al	1.00 ± 0.00	1.00 ± 0.00	1.00 ± 0.00	1.00 ± 0.00	1.00 ± 0.00
K	19.8 ± 2.11	39.1 ± 11.0	0.26 ± 0.04	0.93 ± 0.22	1.16 ± 0.22
Ca	7.87 ± 1.97	8.07 ± 2.00	10.6 ± 2.01	6.99 ± 1.75	4.59 ± 1.00
Sc	0.13 ± 0.04	0.13 ± 0.04	0.05 ± 0.01	0.07 ± 0.02	0.10 ± 0.03
V	0.12 ± 0.04	0.13 ± 0.04	0.05 ± 0.02	0.09 ± 0.02	0.09 ± 0.02
Cr	0.12 ± 0.03	0.12 ± 0.03	0.15 ± 0.04	0.28 ± 0.08	0.13 ± 0.04
Mn	0.13 ± 0.04	0.33 ± 0.08	0.06 ± 0.01	0.19 ± 0.05	0.11 ± 0.03
Fe	0.79 ± 0.18	1.07 ± 0.25	0.85 ± 0.22	1.52 ± 0.38	0.96 ± 0.20
Co	0.11 ± 0.03	0.76 ± 0.18	0.09 ± 0.02	0.58 ± 0.15	0.14 ± 0.04
Ni	0.11 ± 0.03	0.35 ± 0.11	0.33 ± 0.11	0.23 ± 0.05	0.17 ± 0.04
Cu	0.53 ± 0.14	0.76 ± 0.16	114 ± 28.3	4.87 ± 1.01	4.95 ± 1.25
Zn	0.34 ± 0.12	0.57 ± 0.16	6.24 ± 1.85	4.55 ± 1.13	1.36 ± 0.46
As	0.10 ± 0.03	1.50 ± 0.35	1.58 ± 0.45	0.17 ± 0.04	0.13 ± 0.03
Sr	0.78 ± 0.20	0.56 ± 0.16	0.21 ± 0.05	0.48 ± 0.10	0.17 ± 0.04
Cd	0.43 ± 0.12	2.66 ± 0.84	12.7 ± 3.65	51.5 ± 13.2	26.1 ± 8.94
Sn	0.21 ± 0.05	0.36 ± 0.12	19.5 ± 4.17	14.0 ± 3.02	3.70 ± 1.10
Sb	0.16 ± 0.04	0.41 ± 0.15	160 ± 40.1	5.08 ± 1.65	6.93 ± 1.56
Ba	0.16 ± 0.04	0.21 ± 0.05	1.81 ± 0.50	0.43 ± 0.18	0.48 ± 0.15
Tl	0.20 ± 0.05	0.25 ± 0.05	0.48 ± 0.13	0.37 ± 0.11	0.61 ± 0.17
Pb	0.23 ± 0.05	0.69 ± 0.23	26.5 ± 7.70	2.63 ± 0.80	1.30 ± 0.42

Table 3. Igeo values of inorganic elements from 5 combustion sources.

Element	PS	WS	WCC	GFPP	DG
Li	–0.65 ± 0.15	–1.33 ± 0.40	1.20 ± 0.25	–0.22 ± 0.05	–1.06 ± 0.25
Be	–1.28 ± 0.45	–2.22 ± 0.51	–2.28 ± 0.58	–0.61 ± 0.15	–1.74 ± 0.48
Na	2.76 ± 0.85	1.56 ± 0.49	0.53 ± 0.19	3.42 ± 1.05	2.56 ± 0.69
Mg	5.23 ± 1.35	1.34 ± 0.45	3.68 ± 1.16	3.24 ± 1.02	1.03 ± 0.25
Al	1.83 ± 0.53	0.71 ± 0.14	2.34 ± 0.69	2.77 ± 0.56	1.42 ± 0.32
K	5.12 ± 1.31	5.99 ± 1.33	0.37 ± 0.08	2.67 ± 0.65	1.63 ± 0.68
Ca	4.81 ± 1.28	3.72 ± 1.19	5.74 ± 1.38	5.58 ± 1.52	3.61 ± 1.09
Sc	–1.10 ± 0.25	–2.13 ± 0.55	–2.05 ± 0.52	–1.02 ± 0.25	–1.87 ± 0.50
V	–1.19 ± 0.29	–2.28 ± 0.42	–1.87 ± 0.45	–0.77 ± 0.17	–2.06 ± 0.54
Cr	–1.25 ± 0.31	–2.35 ± 0.52	–0.41 ± 0.11	0.94 ± 0.22	–1.51 ± 0.42
Mn	–1.07 ± 0.25	–0.90 ± 0.19	–1.63 ± 0.41	0.35 ± 0.01	–1.76 ± 0.46
Fe	1.49 ± 0.39	0.81 ± 0.26	2.10 ± 0.57	3.37 ± 1.02	1.36 ± 0.38
Co	–1.35 ± 0.41	0.31 ± 0.07	–1.08 ± 0.26	1.99 ± 0.51	–1.33 ± 0.47
Ni	–1.28 ± 0.32	–0.79 ± 0.21	0.75 ± 0.19	0.63 ± 0.15	–1.08 ± 0.24
Cu	0.93 ± 0.22	0.31 ± 0.07	9.18 ± 2.44	5.05 ± 1.53	3.72 ± 1.09
Zn	0.30 ± 0.07	–0.10 ± 0.02	4.98 ± 1.22	4.96 ± 1.21	1.86 ± 0.46
As	–1.54 ± 0.59	1.29 ± 0.31	3.00 ± 0.87	0.19 ± 0.04	–1.57 ± 0.43
Sr	1.48 ± 0.40	–0.13 ± 0.04	0.06 ± 0.02	1.71 ± 0.43	–1.12 ± 0.34
Cd	0.62 ± 0.15	2.12 ± 0.55	6.01 ± 1.25	8.46 ± 2.22	6.12 ± 1.37
Sn	–0.40 ± 0.10	–0.75 ± 0.15	6.63 ± 1.93	6.57 ± 1.86	3.30 ± 1.02
Sb	–0.79 ± 0.26	–0.59 ± 0.15	9.66 ± 3.01	5.12 ± 1.52	4.21 ± 1.27
Ba	–0.86 ± 0.24	–1.52 ± 0.42	3.20 ± 1.00	1.55 ± 0.48	0.38 ± 0.11
Tl	–0.48 ± 0.12	–1.28 ± 0.32	1.29 ± 0.36	1.34 ± 0.38	0.70 ± 0.20
Pb	–0.31 ± 0.07	0.18 ± 0.04	7.07 ± 2.11	4.17 ± 1.12	1.80 ± 0.45

$$DAD_{derm} = \frac{C \times SA \times AF \times ABS}{BW} \times \frac{EF \times ED}{AT} \times CF \quad (6)$$

$$EC_{inh} = C \times ET \frac{EF \times ED}{AT_n} \quad (7)$$

where,
C: the upper bound confidence limit (UCL) for the arithmetic average concentration of metals and As was used as C to obtain the estimate of "reasonable maximum exposure" (Zhang *et al*., 2015b); IngR: provided by U.S. EPA (1989) for the risk assessment of ingestion of soil/dust; BW: average body weight (kg); EF: exposure rate; ED: exposure duration (6 years for children and 24 years for adults) (U.S. EPA, 2014); AT: averaging time (70 years × 365 days year^{-1} for carcinogens and ED × 365 days year^{-1} for non-carcinogens); CF: conversation factor (10^{-6} kg mg^{-1}); SA: surface area contacted by airborne particles; AF: adherence factor of skin; ABS: dermal adsorption factor; ET: exposure time (24 h day^{-1}); and AT_n is average time.

Risk posed by pollutants was classified into carcinogenic and non-carcinogenic effects (Hu *et al.*, 2012).

The cancer risk (CR) is defined as "the incremental probability of an individual developing cancer over a lifetime as a result of exposure to the potential carcinogen" (U.S. EPA, 1989). CR posed by As and heavy metals via inhalation, dermal adsorption, and ingestion was calculated as Eqs. (8)–(10).

$$CR_{ing} = CDI_{ing} \times SFo \quad (8)$$

$$CR_{derm} = \frac{DAD_{derm} \times SFo}{GIABS} \quad (9)$$

$$CD_{inh} = IUR \times EC_{inh} \quad (10)$$

The non-carcinogenic risk (NCR) posed by As and heavy metals was calculated using following expressions.

$$HQ_{ing} = \frac{CDI_{ing}}{RfDo} \quad (11)$$

$$HQ_{derm} = \frac{DAD_{derm} \times RfDo}{GIABS} \quad (12)$$

$$HQ_{inh} = \frac{EC_{inh}}{RfCi \times 1000\ \mu g\ mg^{-1}} \quad (13)$$

where, SFo is oral slope factor ((mg kg·day^{-1})$^{-1}$); GIABS is gastrointestinal adsorption factor; IUR is inhalation unit risk ((μg m^{-3})$^{-1}$); RfDo is oral reference dose ((mg kg·day^{-1})$^{-1}$); and RfCi is inhalation reference concentration (mg m^{-3}).

The integrated carcinogenic and non-carcinogenic exposure risks posed by $PM_{2.5}$ associated heavy metals and As were listed in Fig. 8. Owning to the lack of the data related to air $PM_{2.5}$ concentrations, only two exposure pathways including ingestion (ING) and dermal adsorption (DERM) were involved in this study.

For the carcinogenic risks (CRs) to adults posed by the ING of HMs and As, they were 2.58×10^{-5} for WCC > 9.86

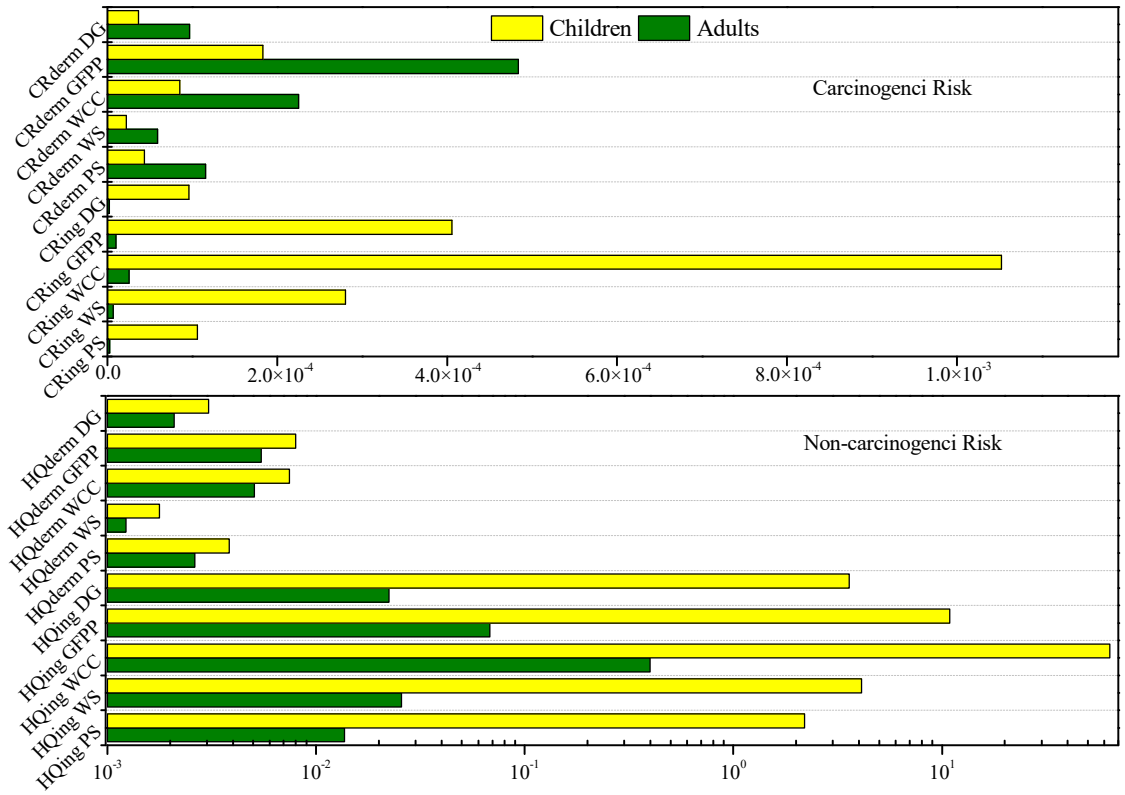

Fig. 8. Integrated carcinogenic and non-carcinogenic exposure risks of $PM_{2.5}$ associated HMs and As.

$\times 10^{-6}$ for GFPP > 6.81×10^{-6} for WS > 2.58×10^{-6} for PS > 2.34×10^{-6} for DG. All the CRs for adults posed by the ING of HMs and As were lower than the acceptable level of 1×10^{-4} designated by US EPA (U.S. EPA, 2011). The CRs for children posed by ING for 4 out of 5 combustion sources were all higher than the acceptable level of 1×10^{-4}, which were 1.05×10^{-3} for WCC > 4.05×10^{-4} for GFPP > 2.80×10^{-4} for WS > 1.06×10^{-4} for PS. The CRs to adults posed by DERM for five sources were all higher than those for children. The CRs for adults posed by DERM of $PM_{2.5}$ associated HMs and As from PS, WCC, and GFPP were all higher than the accepted level of 1×10^{-4}. WCC possessed the highest CRs for children and adults posed by ING, while the highest CRs posed by DERM were owned by GFPP.

The non-carcinogenic risks (NCRs) for children posed by both ING and DERM for all the five sources were much higher than those for adults. The NCRs for adults posed by both ING and DERM were all lower than safe level of 1, the similar trend occurred at NCRs for children through DERM, while the NCRs for children posed by ING were much higher than 1. WCC possessed the highest NCR (63.8) for children derived from ING, which were much higher than those found for GFPP (10.9), WS (4.11), DG (3.58), and PS (2.19).

Table 4 listed the elements with high exposure CRs. The element Cr from WCC and GFPP resulted in higher CRs than 1×10^{-4} for children through ING and for adults through DERM. As from WS and WCC, and Pb from WCC contributed to higher CRs than 1×10^{-4} for children through ING, while Cr from PS could lead to higher CR for adults through DERM.

Table 5 listed the elements with high exposure NCRs. All the NCRs for adults posed by individual IE exposure were lower than the safe level of 1. However, the NCRs for children posed by Co from GFPP, Cu from WCC, As from WS and WCC, Sb from WCC, GFPP, and DG, Tl from WCC and GFPP exceeded the threshold value of 1. Among the aforementioned elements, the maximum value of NCRs was owned by As from WCC (6.96), while the minimum value was attributed to Tl from WCC (1.05). The NCRs for children of the rest of them followed the order Cu from WCC (6.07) > Sb from WCC (4.73) > Sb from GFPP (2.13) > As from WS (2.13) > Tl from GFPP (1.17) > Sb from DG (1.08).

CONCLUSIONS

The burning residues were sampled from the biomass fuels produced in Hebei Province including the peanut straw (PS, n = 4) and wheat stalk (WS, n = 4), workshops of cable combustion (WCC) for metal reclamation in Hebei Province and Tianjin city (n = 3), domestic garbage for its reduction in Hebei Province (DG, n = 3), and garbage-fired power plants (GFPP, n = 4) in Hebei- and Shaanxi- Province during January to May, 2015.

GFPP possessed the highest $\sum_{16}$PAHs as 66500 ± 9800 ng g^{-1}, while the minimum occurred at DG and it is 2480 ng g^{-1}. BaP dominated in GFPP (10600 ng g^{-1}), which should be paid more attention by local government. TEQ values (in ng g^{-1}) for the 5 sources based on TCDD and BaP associated TEFs were GFPP (15500) > WCC (761) > DG (332) > WS (109) > PS (94.3) and GFPP (15400) > WCC (778) > DG (336) > WS (119) > PS (97.2). High contents of

Table 4. Carcinogenic risks for children and adults posed by the individual IE exposure.

Element	CR_{ing}		CR_{derm}		Integrated Risk	
	Children	Adults	Children	Adults	Children	Adults
Cr PS	7.06×10^{-5}	1.72×10^{-6}	4.35×10^{-5}	$\mathbf{1.15 \times 10^{-4}}$	$\mathbf{1.14 \times 10^{-4}}$	$\mathbf{1.17 \times 10^{-4}}$
Cr WS	3.31×10^{-5}	8.05×10^{-7}	2.04×10^{-5}	5.39×10^{-5}	5.35×10^{-5}	5.47×10^{-5}
Cr WCC	$\mathbf{1.26 \times 10^{-4}}$	3.07×10^{-6}	7.78×10^{-5}	$\mathbf{2.06 \times 10^{-4}}$	$\mathbf{2.04 \times 10^{-4}}$	$\mathbf{2.09 \times 10^{-4}}$
Cr GFPP	$\mathbf{2.96 \times 10^{-4}}$	7.19×10^{-6}	1.82×10^{-4}	$\mathbf{4.81 \times 10^{-4}}$	$\mathbf{4.78 \times 10^{-4}}$	$\mathbf{4.88 \times 10^{-4}}$
Cr DG	5.90×10^{-5}	1.43×10^{-6}	3.63×10^{-5}	9.59×10^{-5}	9.53×10^{-5}	9.74×10^{-5}
As PS	3.47×10^{-5}	8.43×10^{-7}	2.77×10^{-7}	7.33×10^{-7}	3.50×10^{-5}	1.58×10^{-6}
As WS	$\mathbf{2.46 \times 10^{-4}}$	5.98×10^{-6}	1.97×10^{-6}	5.21×10^{-6}	$\mathbf{2.48 \times 10^{-4}}$	1.12×10^{-5}
As WCC	$\mathbf{8.05 \times 10^{-4}}$	1.96×10^{-5}	6.44×10^{-6}	1.70×10^{-5}	$\mathbf{8.11 \times 10^{-4}}$	3.66×10^{-5}
As GFPP	9.35×10^{-5}	2.27×10^{-6}	7.48×10^{-7}	1.98×10^{-6}	9.42×10^{-5}	4.25×10^{-6}
As DG	3.40×10^{-5}	8.26×10^{-7}	2.72×10^{-7}	7.18×10^{-7}	3.42×10^{-5}	1.54×10^{-6}
Pb PS	7.28×10^{-7}	1.77×10^{-8}	5.82×10^{-9}	1.54×10^{-8}	7.34×10^{-7}	3.31×10^{-8}
Pb WS	1.02×10^{-6}	2.48×10^{-8}	8.16×10^{-9}	2.16×10^{-8}	1.03×10^{-6}	4.63×10^{-8}
Pb WCC	$\mathbf{1.21 \times 10^{-4}}$	2.94×10^{-6}	9.67×10^{-7}	2.56×10^{-6}	$\mathbf{1.22 \times 10^{-4}}$	5.50×10^{-6}
Pb GFPP	1.61×10^{-5}	3.91×10^{-7}	1.29×10^{-7}	3.40×10^{-7}	1.62×10^{-5}	7.32×10^{-7}
Pb DG	3.13×10^{-6}	7.61×10^{-8}	2.51×10^{-8}	6.62×10^{-8}	3.16×10^{-6}	1.42×10^{-7}

Table 5. The elements with high exposure non-carcinogenic risks to adults and children.

Elements	HQ_{ing}		HQ_{derm}		Integrated Risk	
	Children	Adults	Children	Adults	Children	Adults
Co PS	3.12×10^{-1}	1.95×10^{-3}	2.25×10^{-10}	1.53×10^{-10}	3.12×10^{-1}	1.95×10^{-3}
Co WS	9.82×10^{-1}	6.14×10^{-3}	7.07×10^{-10}	4.81×10^{-10}	9.82×10^{-1}	6.14×10^{-3}
Co WCC	3.74×10^{-1}	2.34×10^{-3}	2.70×10^{-10}	1.83×10^{-10}	3.74×10^{-1}	2.34×10^{-3}
Co GFPP	$\mathbf{2.68 \times 10^{0}}$	1.68×10^{-2}	1.93×10^{-9}	1.31×10^{-9}	$\mathbf{2.68 \times 10^{0}}$	1.68×10^{-2}
Co DG	3.16×10^{-1}	1.98×10^{-3}	2.28×10^{-9}	1.55×10^{-10}	3.16×10^{-1}	1.98×10^{-3}
Cu PS	1.99×10^{-2}	1.24×10^{-4}	2.54×10^{-7}	1.73×10^{-7}	1.99×10^{-2}	1.24×10^{-4}
Cu WS	1.29×10^{-2}	8.08×10^{-5}	1.65×10^{-7}	1.12×10^{-7}	1.29×10^{-2}	8.09×10^{-5}
Cu WCC	$\mathbf{6.07 \times 10^{0}}$	3.79×10^{-2}	7.76×10^{-5}	5.28×10^{-5}	$\mathbf{6.07 \times 10^{0}}$	3.80×10^{-2}
Cu GFPP	3.41×10^{-1}	2.13×10^{-3}	4.36×10^{-6}	2.96×10^{-6}	3.41×10^{-1}	2.13×10^{-3}
Cu DG	1.38×10^{-1}	8.63×10^{-4}	1.77×10^{-6}	1.20×10^{-6}	1.38×10^{-1}	8.64×10^{-4}
As PS	3.00×10^{-1}	1.87×10^{-3}	2.16×10^{-10}	1.47×10^{-10}	3.00×10^{-1}	1.87×10^{-3}
As WS	$\mathbf{2.13 \times 10^{0}}$	1.33×10^{-2}	1.53×10^{-9}	1.04×10^{-9}	$\mathbf{2.13 \times 10^{0}}$	1.33×10^{-2}
As WCC	$\mathbf{6.96 \times 10^{0}}$	4.35×10^{-2}	5.01×10^{-9}	3.40×10^{-9}	$\mathbf{6.96 \times 10^{0}}$	4.35×10^{-2}
As GFPP	8.08×10^{-1}	5.05×10^{-3}	5.82×10^{-10}	3.95×10^{-10}	8.08×10^{-1}	5.05×10^{-3}
As DG	2.94×10^{-1}	1.83×10^{-3}	2.11×10^{-10}	1.44×10^{-10}	2.94×10^{-1}	1.83×10^{-3}
Sb PS	3.38×10^{-2}	2.11×10^{-4}	2.88×10^{-10}	1.96×10^{-10}	3.38×10^{-2}	2.11×10^{-4}
Sb WS	3.87×10^{-2}	2.42×10^{-4}	3.31×10^{-10}	2.25×10^{-10}	3.87×10^{-2}	2.42×10^{-4}
Sb WCC	$\mathbf{4.73 \times 10^{1}}$	2.95×10^{-1}	4.03×10^{-7}	2.74×10^{-7}	4.73×10^{-1}	2.95×10^{-1}
Sb GFPP	$\mathbf{2.23 \times 10^{0}}$	1.39×10^{-2}	1.90×10^{-8}	1.29×10^{-8}	$\mathbf{2.23 \times 10^{0}}$	1.39×10^{-2}
Sb DG	$\mathbf{1.08 \times 10^{0}}$	6.76×10^{-3}	9.23×10^{-9}	6.27×10^{-9}	$\mathbf{1.08 \times 10^{0}}$	6.76×10^{-3}
Tl PS	3.07×10^{-1}	1.92×10^{-3}	9.82×10^{-13}	6.67×10^{-13}	3.07×10^{-1}	1.92×10^{-3}
Tl WS	1.76×10^{-1}	1.10×10^{-3}	5.65×10^{-13}	3.84×10^{-13}	1.76×10^{-1}	1.10×10^{-3}
Tl WCC	$\mathbf{1.05 \times 10^{0}}$	6.57×10^{-3}	3.36×10^{-12}	2.29×10^{-12}	$\mathbf{1.05 \times 10^{0}}$	6.57×10^{-3}
Tl GFPP	$\mathbf{1.17 \times 10^{0}}$	7.29×10^{-3}	3.73×10^{-12}	2.54×10^{-12}	$\mathbf{1.17 \times 10^{0}}$	7.29×10^{-3}
Tl DG	6.98×10^{-1}	4.36×10^{-3}	2.23×10^{-12}	1.52×10^{-12}	6.98×10^{-1}	4.36×10^{-3}

BaP in GFPP and DG combined with high TEF values might be the explanations. In regard to the BaPE (in ng g^{-1}), the same trend with both TEQ and BaPeq was found, which was GFPP (13600) > WCC (656) > DG (303) > WS (82.9) > PS (79.4).

The sum of 10 HMs and As ($\sum_{11}$IEs) dominated in WCC resulted from its high contents of Cu, Zn, and Pb (23.4 ± 2.88 mg g^{-1}). The Σ_{11}IEs followed the order as GFPP (5.44 ± 0.65 mg g^{-1}) > DG (1.16 ± 0.06 mg g^{-1}) > WS (0.68 ± 0.09 mg g^{-1}) > PS (0.63 ± 0.05 mg g^{-1}). Only one lower CD value than 0.3 was found for GFPP vs. DG, the rest pairs of sources possessed higher CD values than 0.3 and they were 0.36 for PS vs. WS, 0.72 for PS vs. WCC, 0.55 for PS vs. GFPP, 0.51 for PS vs. DG, 0.76 for WS vs. WCC, 0.60 for WS vs. GFPP, 0.58 for WS vs. DG, 0.68 for WCC vs. GFPP, and 0.67 for WCC vs. DG.

According to the enrichment factors of IEs, K was more enriched in biomass fuel such as PS and WS, Sb, Cu, and Pb

were more inclined to enrich in WCC, Sn was preferential enrichment in WCC and GFPP, and Cd intended to enrich in GFPP and DG. Sb and Cu in WCC possess higher EF values as 160 and 114, which suggested the significant influence of human activities. Sb, Cu, Pb, Sn, and Cd in $PM_{2.5}$ from WCC owned the Igeo values as high as 9.66, 9.18, 7.07, 6.63, and 6.01, Cd, Sn, Sb, and Cu from GFPP possessed Igeo values as 8.46, 6.57, 5.12, and 5.05, and Cd from DG also possessed high Igeo value as 6.12, which indicated these HMs were extremely contamination.

The carcinogenic risks (CRs) for adults posed by dermal adsorption (DERM) were higher than those for children, while the reverse trend was found for CRs posed by ingestion (ING). The CRs for adults posed by ING of HMs and As from all the 5 sources were lower than the safety limit of 1×10^{-4}, which were 2.58×10^{-5} for WCC > 9.86×10^{-6} for GFPP > 6.81×10^{-6} for WS > 2.58×10^{-6} for PS > 2.34×10^{-6} for DG. However, the CRs for children posed by ING of HMs and As from 4 sources exceeded the acceptable level, and they were 1.05×10^{-3} for WCC, 4.05×10^{-4} for GFPP, 2.08×10^{-4} for WS, and 1.06×10^{-4} for PS, respectively. The non-carcinogenic risks (NCRs) for children posed by both ING and DERM for all the five sources were much higher than those for adults. Both NCRs for adults posed by ING and DERM, and NCRs for children through DERM were lower than the acceptable level of 1, while the NCRs for children by ING were much higher than 1. WCC possessed the highest NCR (63.8) for children derived from ING, which were much higher than those found for GFPP (10.9), WS (4.11), DG (3.58), and PS (2.19).

ACKNOWLEDGEMENTS

This study was supported by the Fundamental Research Funds for the Central Universities (2017MS142), the National Natural Science Foundation of China (21407048), and Prime Minister Fund (DQGG-05-13).

REFERENCES

Abbas, I., Badran, G., Verdin, A., Ledoux, F., Roumie, M. and Courcot, D. (2018). Polycyclic aromatic hydrocarbon derivatives in airborne particulate matter: Sources, analysis and toxicity. *Environ. Chem. Lett*. 16: 439–475.

Bamai, Y.A., Araki, A., Kawai, T., Tsuboi, T., Saito, I., Yoshioka, E., Cong, S. and Kishi, R. (2016). Exposure to phthalates in house dust and associated allergies in children aged 6-12 years. *Environ. Int.* 96: 16–23.

Bond, T.C., Streets, D.G., Yarber, K.F., Nelson, S.M., Woo, J.H. and Klimont, Z. (2004). A technology-based global inventory of black and organic carbon emissions from combustion. *J. Geophys.* Res. 109: D14203.

Chan, Y.J., Yuan, T.H., Sun, H.C. and Lin, T.C. (2016). Characterization and exposure assessment of odor emissions from laser cutting of plastics in the optical film industry. *Aerosol Air Qual. Res.* 16: 2216–2226.

Chen, P.F., Kang, S.C., Li, C.L., Li, Q.L., Yan, F.P., Guo, J.M., Ji, Z.M., Zhang, Q.G., Hu, Z.F., Tripathee, L. and Sillanpää, M. (2018). Source apportionment and risk assessment of atmospheric polycyclic aromatic hydrocarbons in Lhasa, Tibet, China. *Aerosol Air Qual. Res.* 18: 1294–1304.

Cheruiyot, N.K., Lee, W.J., Mwangi, J.K., Wang, L.C., Lin, N.H., Lin, Y.C., Cao, J.J., Zhang, R.J., Guo, P. and Chang, C. (2015). An overview: Polycyclic aromatic hydrocarbon emissions from the stationary and mobile sources and in the ambient air. *Aerosol Air Qual. Res.* 15: 2730–2762.

Consonni, S., Giugliano, M. and Grosso, M. (2005). Alternative strategies for energy recovery from municipal solid waste, Part B: Emission and cost estimates. *Waste Manage*. 25: 137–148.

Dat, N.D., Lyu, J.M. and Chan, M.B. (2018). Variation of atmospheric PAHs in Northern Taiwan during winter and summer seasons. *Aerosol Air Qual. Res.* 18: 1019–1031.

Elzein, A., Dunmore, R.E., Ward, M.W., Hamilton, J.F. and Lewis, A.C. (2019). Variability of polycyclic aromatic hydrocarbons and their oxidative derivatives in wintertime Beijing, China. *Atmos. Chem. Phys.* 19: 8741–8758.

Fang, M., Chan, C. and Yao, X. (2009). Managing air quality in a rapidly developing nation: China. *Atmos. Environ.* 43: 79–86.

Hamra, G.B., Guha, N., Cohen, A., Laden, F., Raaschou-Nielsen, O., Samet, J.M., Vineis, P., Forastiere, F., Saldiva, P., Yorifuji, T. and Loomis, D. (2014). Outdoor particulate matter exposure and lung cancer: A systematic review and meta-analysis. *Environ. Health Perspect.* 122: 906–911.

Hou, B.D., Tang, X., Ma, C., Liu, L., Wei, Y.M. and Liao, H. (2017). Cooking fuel choice in rural China: Results from microdata. *J. Cleaner Prod.* 142: 538–547.

Hu, X., Zhang, Y., Ding, Z.H., Wang, T.J., Lian, H.Z., Sun, Y.Y. and Wu, J.C. (2012). Bioaccessibility and health risk of arsenic and heavy metals (Cd, Co, Cr, Cu, Ni, Pb, Zn, and Mn) in TSP and $PM_{2.5}$ in Nanjing, China. *Atmos. Environ.* 57: 146–152.

Hu, Y., Li, Z.Y., Wang, L., Zhu, H.T., Chen, L., Guo, X.B., An, C.X., Jiang, Y.J. and Liu, A.Q. (2019). Emission factors of NO_x, SO_2, PM and VOCs in pharmaceuticals, brick and food industries in Shanxi, China. *Aerosol Air Qual. Res.* 19: 1785–1797.

Huang, C.W., Miyata, H., Lu, J.R., Ohta, S., Chang, T. and Kashimoto, T. (1992). Levels of PCBs, PCDDs and PCDFs in soil samples from incineration sites for metal reclamation in Taiwan. *Chemosphere* 24: 1669–1676.

Kong, S.F., Shi, J.W., Lu, B., Qiu, W.G., Zhang, B.S., Peng, Y., Zhang, B.W. and Bai, Z.P. (2011). Characterization of PAHs within PM_{10} fraction for ashes from coke production, iron smelt, heating station and power plant stacks in Liaoning Province, China. *Atmos. Environ*. 45: 3777–3785.

Košnář, Z., Mercl, F., Perná, I. and Tlustoš, P. (2016). Investigation of polycyclic aromatic hydrocarbon content in fly ash and bottom ash of biomass incineration plants in relation to the operating temperature and unburned carbon content. *Sci. Total Environ.* 563–564: 53–61.

Li, Z.Y., Kong, S.F., Chen, L., Bai, Z.P., Ji, Y.Q., Liu, J.W., Lu, B., Han, B. and Wang, Q.W. (2011). Concentrations, spatial distributions and congener profiles of polychlorinated biphenyls in soils from a coastal city-Tianjin, China.

Chemosphere 85: 494–501.

Li, Z.Y., Chen, L., Liu, S.T., Ma, H.Q., Wang, L., An, C.X. and Zhang, R.L. (2016). Characterization of PAHs and PCBs in fly ashes of eighteen coal-fired power plants. *Aerosol Air Qual. Res.* 16: 3175–3186.

Li, Z.Y., Ji, Y.Q., Ma, H.Q., Zhao, P., Zeng, X.C., Liu, S.T., Jiang, Y.J., Wang, L., Liu, A.Q., Gao, H.Y., Liu, F.D. and Mwangi, J.K. (2017a). Characterization of inorganic elements within $PM_{2.5}$ and PM_{10} fractions of fly ashes from coal-fired power plants. *Aerosol Air Qual. Res.* 17: 1105–1116.

Li, Z.Y., Ma, H.Q., Fan, L., Zhao, P., Wang, L., Jiang, Y.J., An, C.X., Liu, A.Q., Hu, Z.S. and Jin, H. (2017b). Size distribution of inorganic elements in bottom ashes from seven types of bio-fuels across Beijing-Tianjin-Hebei region, China. *Aerosol Air Qual. Res.* 17: 2450–2462.

Li, Z.Y., Fan, L., Wang, L., Ma, H.Q., Hu, Y., Jiang, Y.J., An, C.X., Liu, A.Q., Han, J.B. and Jin, H. (2018a). PAH profiles of emitted ashes from indoor biomass burning across the Beijing-Tianjin-Hebei region and implications on source identification. *Aerosol Air Qual. Res.* 18: 749–761.

Li, Z.Y., Hu, Y., Chen, L., Wang, L., Fu, D., Ma, H.Q., Fan, L., An, C.X. and Liu, A.Q. (2018b). Emission factors of NO_x, SO_2, and PM for bathing, heating, power generation, coking, and cement industries in Shanxi, China: Based on field measurement. *Aerosol Air Qual. Res.* 18: 3115–3126.

Liu, H. (2015). Analysis of discharge standard of pollutants for garbage incineration power plant. *Environ. Dev. Sustainability* 40: 73–74.

Liu, J., Zhao J.P., Yang, L.H., Huang, D.J., Wang, X., Deng, D.Y. and Han, J.L. (2016). Inhalation exposure risk assessment of a typical municipal solid waste incinerator, South China. *Ecol. Environ. Sci.* 25: 440–446. (in Chinese)

Liu, W.X., Dou, H., Wei, Z.C., Chang, B., Qiu, W.X., Liu, Y. and Tao, S. (2009). Emission characteristics of polycyclic aromatic hydrocarbons from combustion of different residential coals in North China. *Sci. Total Environ*. 407: 1436–1446.

Mario, A., Mihaela, M., Massimo, D.I. and Maurizio, G. (2018). Impact of emissions, meteorology and grid resolution on changes in HMs and PAHs concentrations between 2005 and 2010 in Italy. *Aerosol Air Qual. Res.* 18: 3165–3176.

Masto, R.E., Sarkar, E., George, J., Jyoti, K., Dutta, P. and Ram, L.C. (2015). PAHs and potentially toxic elements in the fly ash and bed ash of biomass fired power plants. *Fuel Process. Technol.* 132: 139–152.

Megido, L., Suarez-Pena, B., Negral, L., Castrillon, L. and Fernandez-Nava, Y. (2017). Suburban air quality: Human health hazard assessment of potentially toxic elements in PM_{10}. *Chemosphere* 177: 284–291.

Murphy, J.D. and McKeogh, E. (2004). Technical economic and environmental analysis of energy production from municipal solid waste. *Renewable Energy* 29: 1043–1057.

Nisbet, C. and LaGoy, P. (1992). Toxic equivalence factors (TEFs) for polycyclic aromatic hydrocarbons (PAHs). *Regul. Toxicol. Pharm.* 16: 290–300.

Orecchio, S., Amorello, D., Barreca, S. and Valenti, A. (2016). Wood pellets for home heating can be considered environmentally friendly fuels? Polycyclic aromatic hydrocarbons (PAHs) in their ashes. *Microchem. J.* 124: 267–271.

Pascal, M., Corso, M., Chanel, O., Declercq, C., Badaloni, C., Cesaroni, G., Henschel, S., Meister, K., Haluza, D., Martin-Olmedo, P. and Medina, S. (2013). Assessing the public health impacts of urban air pollution in 25 European cities: Results of the Aphekom project. *Sci. Total Environ*. 449: 390–400.

Peng, N.N., Li, Y., Liu, Z.G., Liu, T.T. and Gai, C. (2016a). Emission, distribution and toxicity of polycyclic aromatic hydrocarbons (PAHs) during municipal solid waste (MSW) and coal co-combustion. *Sci. Total Environ.* 565: 1201–1207.

Peng, N.N., Liu, Z.G., Liu, T.T. and Gai, C. (2016b). Emissions of polycyclic aromatic hydrocarbons (PAHs) during hydrothermally treated municipal solid waste combustion for energy generation. *Appl. Energy* 184: 396–403.

Saikawa, E., Naik, V., Horowitz, L.W., Liu, J.F. and Mauzerall, D.L. (2009). Present and potential future contributions of sulfate, black and organic carbon aerosols from China to global air quality, premature mortality and radiative forcing. *Atmos. Environ.* 43: 2814–2822.

Singh, D.P., Gadi, R., Mandal, T.K., Saud, T., Saxena, M.A. and Sharma, S.K. (2013). Emission estimates of PAH from biomass fuels used in rural sector of indogangetic plains of India. *Atmos. Environ*. 68: 120–126.

Tiwari, M., Sahu, S.K. and Pandit, G.G. (2017). PAHs in size fractionate mainstream cigarette smoke, predictive deposition and associated inhalation risk. *Aerosol Air Qual. Res.* 17: 176–186.

U.S. EPA (1989). Risk Assessment Guidance for Superfund: Volume I - Human Health Evaluation Manual (Part A) (Interim Final). EPA/540/1-89/002. Office of Emergency and Remedial Response, U.S. Environmental Protection Agency, Washington, D.C., USA.

U.S. EPA (2009). Risk Assessment Guidance for Superfund Volume I: Human Health Evaluation Manual (Part F, Supplemental Guidance for Inhalation Risk Assessment) (Final). EPA-540-R-070-002. OSWER 9285.7-82. Office of Superfund Remediation and Technology Innovation, U.S. Environmental Protection Agency, Washington, D.C., USA.

U.S. EPA (2011). Risk Assessment Guidance for Superfund. In: Part A: Human Health Evaluation Manual; Part E, Supplemental Guidance for Dermal Risk Assessment; Part F, Supplemental Guidance for Inhalation Risk Assessment, Vol. I. http://www.epa.gov/oswer/riskassessment/human_health_exposure.htm.

U.S. EPA (2014). Human Health Evaluation Manual, Supplemental Guidance: Update of Standard Default Exposure Factors. U.S. Environmental Protection Agency. https://www.epa.gov/sites/production/files/2015-11/documents/oswer_directive_9200.1-120_exposurefactors _corrected2.pdf.

Valavanidis, A., Iliopoulos, N., Gotsis, G. and Fiotakis, K. (2008). Persistent free radicals, heavy metals and PAHs

generated in particulate soot emissions and residue ash from controlled combustion of common types of plastic. *J. Hazard. Mater.* 156: 277–284.

Wang, J.Z., Dong, Z.B., Li, X.P., Gao, M.L., Ho, S.S.H., Wang, G.H., Xiao, S. and Cao, J.J. (2018). Intra-urban levels, spatial variability, possible sources and health risks of $PM_{2.5}$ bound phthalate esters in Xi'an. *Aerosol Air Qual. Res.* 18: 485–496.

Wang, R.W., Zhang, J.M., Liu, J.J. and Liu, G.J. (2013). Levels and patterns of polycyclic aromatic hydrocarbons in coal-fired power plant bottom ash and fly ash from Huainan, China. *Arch. Environ. Contam. Toxicol.* 65: 193–202.

Wang, Z.Z, Tan, J.H., Bi, X.H., Duan, J.C., Sheng, G.Y. and Fu, J.M. (2016). Emission characteristics and chemical species from agricultural straw burning smoke. *Environ. Sci. Technol*. 11: 150–155. (in Chinese)

Wei, B.G., Jiang, F.Q., Li, X.M. and Mu, S.Y. (2009). Spatial distribution and contamination assessment of heavy metals in urban road dusts from Urumqi, NW China. *Microchem. J.* 93: 147–152.

Wongphatarakul, V., Friedlander, S.K. and Pinto, J.P. (1998). A comparative study of $PM_{2.5}$ ambient aerosol chemical databases. *Environ. Sci. Technol*. 32: 3926–3934.

Xiang, M.D., Yang, L., Yu, Y.J., Ren, M.Z., Li, L.Z. and Sun, J.R. (2013). The study on location selection of municipal solid waste incineration power plant based on health risk assessment. *China Environ. Sci.* 33: 165–171. (in Chinese)

Xu, S.S., Liu, W.X. and Tao, S. (2006). Emission of polycyclic aromatic hydrocarbons in China. *Environ. Sci. Technol.* 40: 702–708.

Zdeněk, K., Mercl, F., Perná, I. and Tlustoš, P. (2016). Investigation of polycyclic aromatic hydrocarbon content in fly ash and bottom ash of biomass incineration plants in relation to the operating temperature and unburned carbon content. *Sci. Total Environ.* 563–564: 53–61.

Zhai, S.X., Jacob, D.J., Wang, X., Shen, L., Li, K., Zhang, Y.Z., Gui, K., Zhao, T.L. and Liao, H. (2019). Fine particulate matter ($PM_{2.5}$) trends in China, 2013-2018: Contributions from meteorology. *Atmos. Chem. Phys.* 19: 11031–11041.

Zhang, N., Han, B., He, F., Xu, J., Zhou, J., Kong, S.F., Bai, Z.P. and Xu, H. (2015b). Characterization, health risk of heavy metals, and source apportionment of atmospheric $PM_{2.5}$ to children in summer and winter: An exposure panel study in Tianjin, China. *Air Qual. Atmos. Health* 28: 347–354.

Zhang, Q., Shen, Z., Cao, J., Zhang, R., Zhang, L., Huang, R.J., Zheng, C., Wang, L., Liu, S., Xu, H., Zheng, C. and Liu, P. (2015a). Variations in $PM_{2.5}$, TSP, BC, and trace gases (NO_2, SO_2, and O_3) between haze and non-haze episodes in winter over Xi'an, China. *Atmos. Environ.* 112: 64–71.

Zhang, Y., Yang, L.X., Zhang, X.F., Li, J.S., Zhao, T., Gao, Y., Jiang, P., Li, Y.Y., Chen, X.F. and Wang, W.X. (2019). Characteristics of $PM_{2.5}$-bound PAHs at an urban site and a suburban site in Jinan in North China Plain. *Aerosol Air Qual. Res.* 19: 871–884.

Zhang, Z.Q., Zhang, M.W., Zhao, B.W., Zhang, S.K. and Ren, M.Z. (2013). Concentrations and profiles of PCDD/Fs in ambient air around a municipal solid waste incinerator. *China Environ. Sci.* 33: 1207–1214. (in Chinese)

Zhou, H.C., Jin, B.S., Xiao, R., Zhong, Z.P. and Huang, Y.J. (2009). Distribution of polycyclic aromatic hydrocarbons in fly ash during coal and residual char combustion in a pressurized fluidized bed. *Energy Fuels* 23: 2031–2034.

Received for review, October 3, 2019
Revised, October 21, 2019
Accepted, October 22, 2019